Supporting information

Mechanism of rate controllability of water-soluble bifunctional cyclooctadiynes through cation-anion interactions

Moeka Yoshinaga,[a] Fumiya Sato,[a] Kohei Kitagawa,[a] Natsuki Yokota,[a] Shogo Sasaki,[a] Manami Takeuchi,[a] Hiroshi Tsugawa,[a] Kohtaro Sugahara,[b] Shoko Mori [b] and Masayuki Tera*[a]

[a.]Department of Biotechnology and Life Science, Tokyo University of Agriculture and Technology, 2-24-16 Naka-cho, Koganei, Tokyo 184-8588, Japan.
E-mail: tera@go.tuat.ac.jp
[b.]Bioorganic Research Institute, Suntory Foundation for Life Sciences, 8-1-1 Seikadai, Seika, Soraku, Kyoto 619-0284, Japan.

Table of Contents

1. General methods and reagents.

Lysozyme (L6876), HSA (A9731) and orosomucoid (G9885) were purchased from Sigma-Aldrich. LC-MS/MS analyses were performed on a ZenoTOF 7600 mass spectrometer (SCIEX) equipped with a Exion liquid chromatography system (SCIEX). NMR spectra were measured with a AVANCE III HD 800 (800 MHz for ^{1}H, 200 MHz for ^{13}C). Chemical shifts (δ) are given in parts per million (ppm) and are reported relative to residual solvent peaks: CD_3OD (δH 3.31, δC.49.00 ppm). Curve fitting was carried out in GraphPad Prism 9. SDS-PAGE images were acquired on ChemiDoc XRS (Bio-Rad). Image analysis was performed using ImageJ (National Institutes of Health, USA).

2. Analysis of reaction rates between WS-CODY and azides.

Rate measurements of the first (rate limiting) cycloaddition reaction were performed under pseudo first order reaction conditions by monitoring changes in the absorbance of solutions containing WS-CODY in the presence of a large excess azides. 60 μL of the solution of WS-CODY (final concentration = **1a**: 0.6 or 1.2 mM, **1b**: 1.0 mM, and **1c**: 0.96 mM in H_2O) or CODY (final concentration = **1d**: 1.0 mM in MeOH) was placed in 96 well plates or a cuvette and 60 μL of azides solution in H_2O (for the reaction with **1a-c**) or MeOH (for the reaction with **1d**) was added to give final azides concentrations ranging from 0-55 mM. The time-dependent consumption of **1a-d** was monitored by the loss in absorbance at 350 nm, a wavelength characteristic absorbance of the diyne. Same protocols as above described were used for the rate measurements in the addition of 100 mM NaCl or $MgSO_4$. The experiments were repeated in triplicate for each concentration of azides.

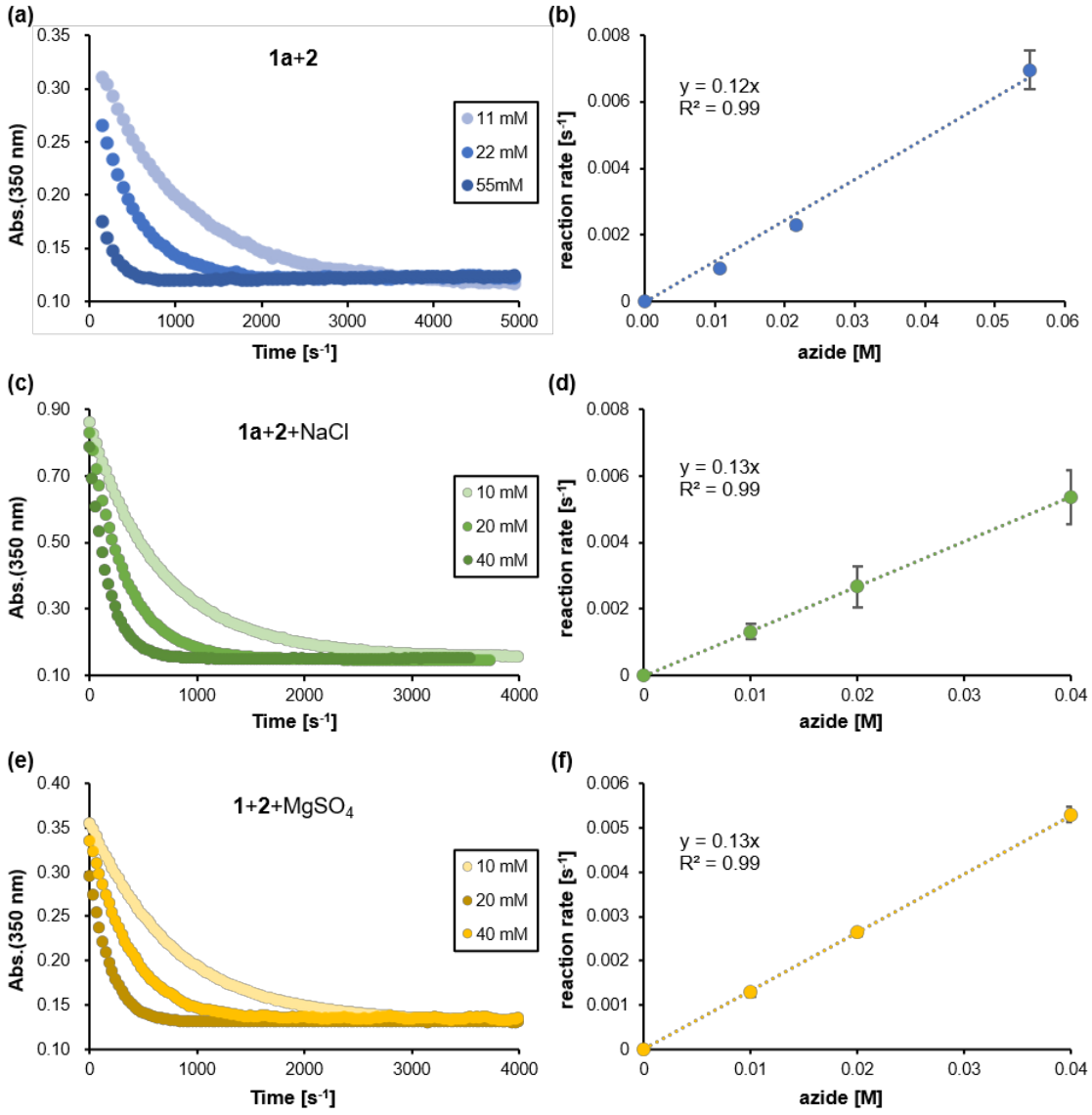

Fig. S1 (a) Normalized first-order exponential decay of DMA-CODY (**1a**) absorbance (350 nm) in the presence of **2** in H_2O at 25 ºC, monitored over time, where [**1a**] = 0.6 mM, and [**2**] = 11, 22 or 55 mM. (b) Linear regression of pseudo-first order rates versus **2** concentrations to derive the apparent second-order rate constant. (c) Normalized first-order exponential decay of **1a** absorbance (350 nm) in the presence of **2** and NaCl in H_2O at 25 ºC, monitored over time, where [**1a**] = 1.2 mM, [**2**] = 10, 20 or 40 mM, and [NaCl] = 100 mM. (d) Linear regression of pseudo-first order rates versus **2** concentrations in the presence of NaCl to derive the apparent second-order rate constant. (e) Normalized first-order exponential decay of **1a** absorbance (350 nm) in the presence of **2** and $MgSO_4$ in H_2O at 25 ºC, monitored over time, where [**1a**] = 1.2 mM, [**2**] = 10, 20 or 40 mM, and [$MgSO_4$] = 100 mM. (f) Linear regression of pseudo-first order rates versus **2** concentrations in the presence of $MgSO_4$ to derive the apparent second-order rate constant. Data represent the mean from three

independent experiments and error bars show standard deviation (SD).

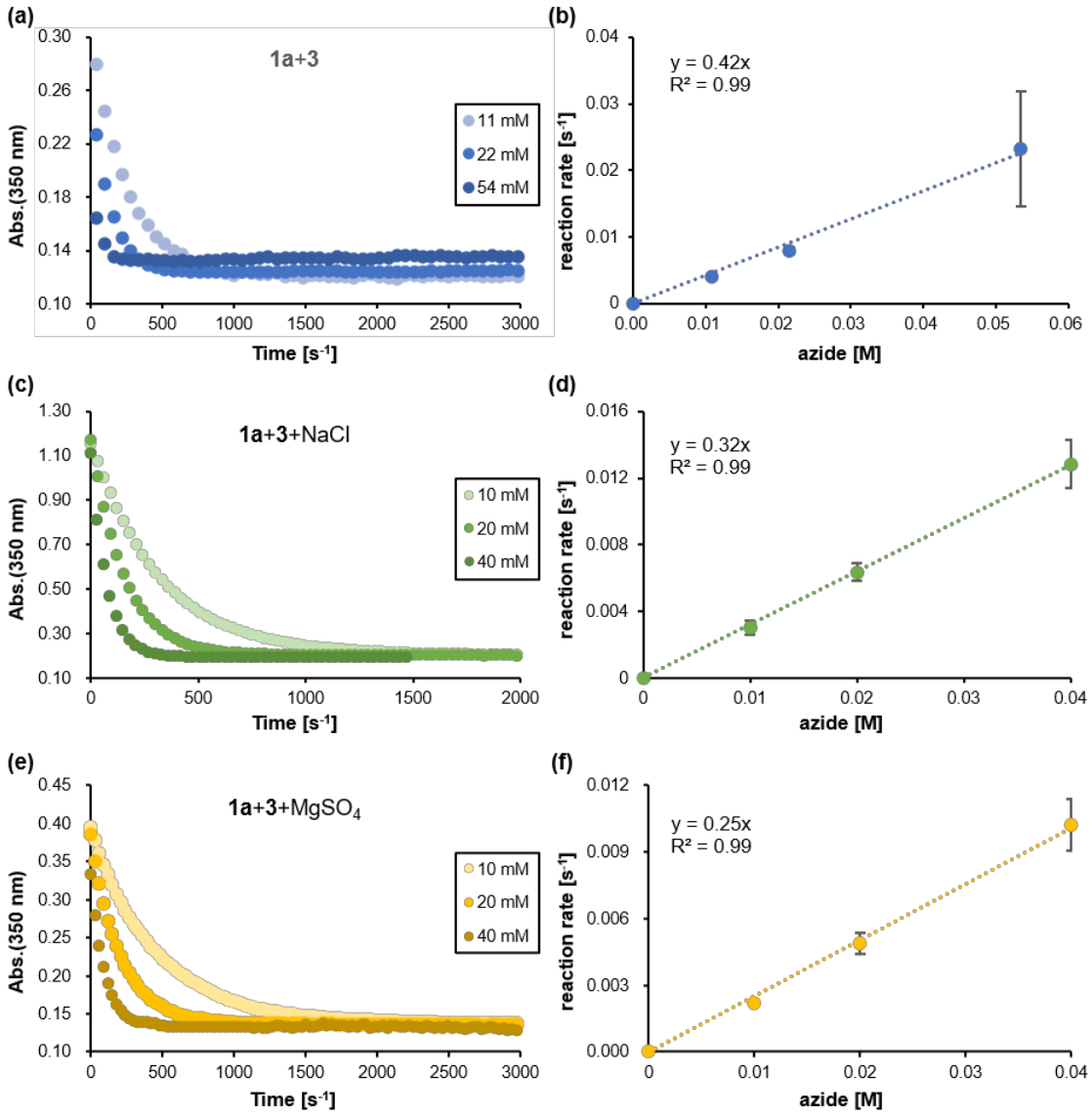

Fig. S2 (a) Normalized first-order exponential decay of DMA-CODY (**1a**) absorbance (350 nm) in the presence of **3** in H_2O at 25 ºC, monitored over time, where [**1a**] = 0.6 mM, and [**3**] = 11, 22 or 54 mM. (b) Linear regression of pseudo-first order rates versus **3** concentrations to derive the apparent second-order rate constant. (c) Normalized first-order exponential decay of **1a** absorbance (350 nm) in the presence of **3** and NaCl in H_2O at 25 ºC, monitored over time, where [**1a**] = 1.2 mM, [**3**] = 10, 20 or 40 mM, and [NaCl] = 100 mM. (d) Linear regression of pseudo-first order rates versus **3** concentrations in the presence of NaCl to derive the apparent second-order rate constant. (e) Normalized first-order exponential decay of **1a** absorbance (350 nm) in the presence of **2** and $MgSO_4$ in H_2O at 25 ºC, monitored over time, where [**1a**] = 1.2 mM, [**3**] = 10, 20 or 40 mM, and [$MgSO_4$] =

100 mM. (f) Linear regression of pseudo-first order rates versus **2** concentrations in the presence of $MgSO_4$ to derive the apparent second-order rate constant. Data represent the mean from three independent experiments and error bars show standard deviation (SD).

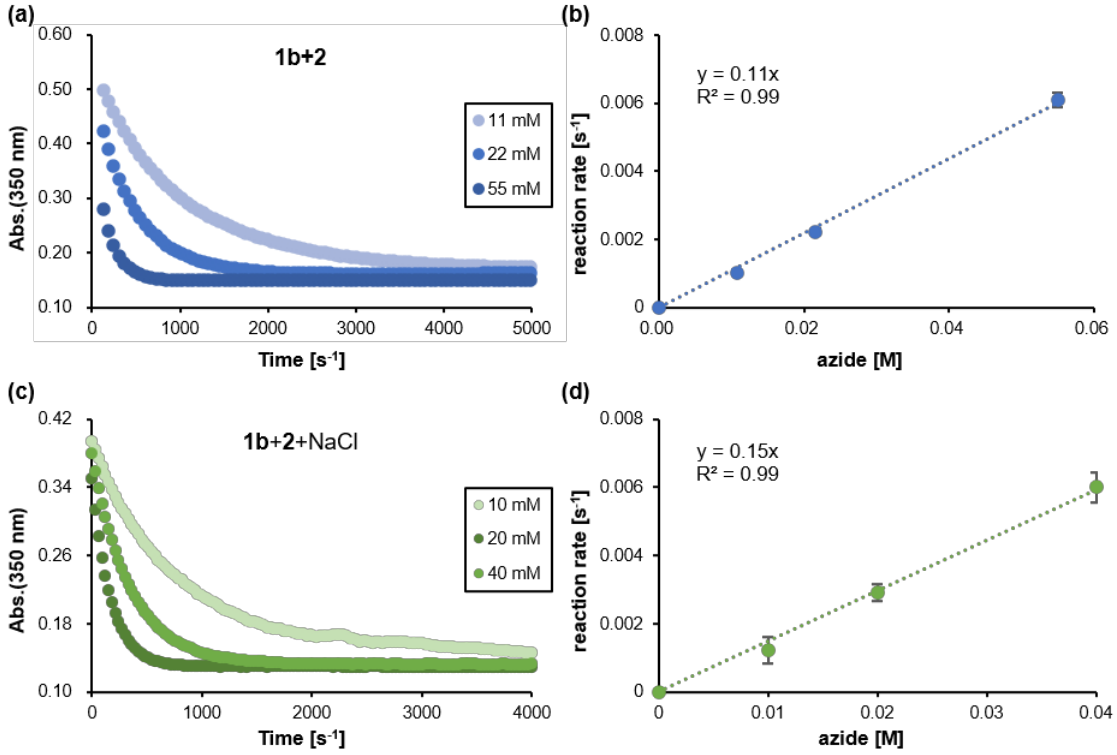

Fig. S3 (a) Normalized first-order exponential decay of DSP-CODY (**1b**) absorbance (350 nm) in the presence of **2** in H_2O at 25 ºC, monitored over time, where [**1b**] = 1.0 mM, and [**2**] = 11, 22 or 55 mM. (b) Linear regression of pseudo-first order rates versus **2** concentrations to derive the apparent second-order rate constant. (c) Normalized first-order exponential decay of **1b** absorbance (350 nm) in the presence of **2** and NaCl in H_2O at 25 ºC, monitored over time, where [**1b**] = 1.0 mM, [**2**] = 10, 20 or 40 mM, and [NaCl] = 100 mM. (d) Linear regression of pseudo-first order rates versus **2** concentrations in the presence of NaCl to derive the apparent second-order rate constant. Data represent the mean from three independent experiments and error bars show standard deviation (SD).

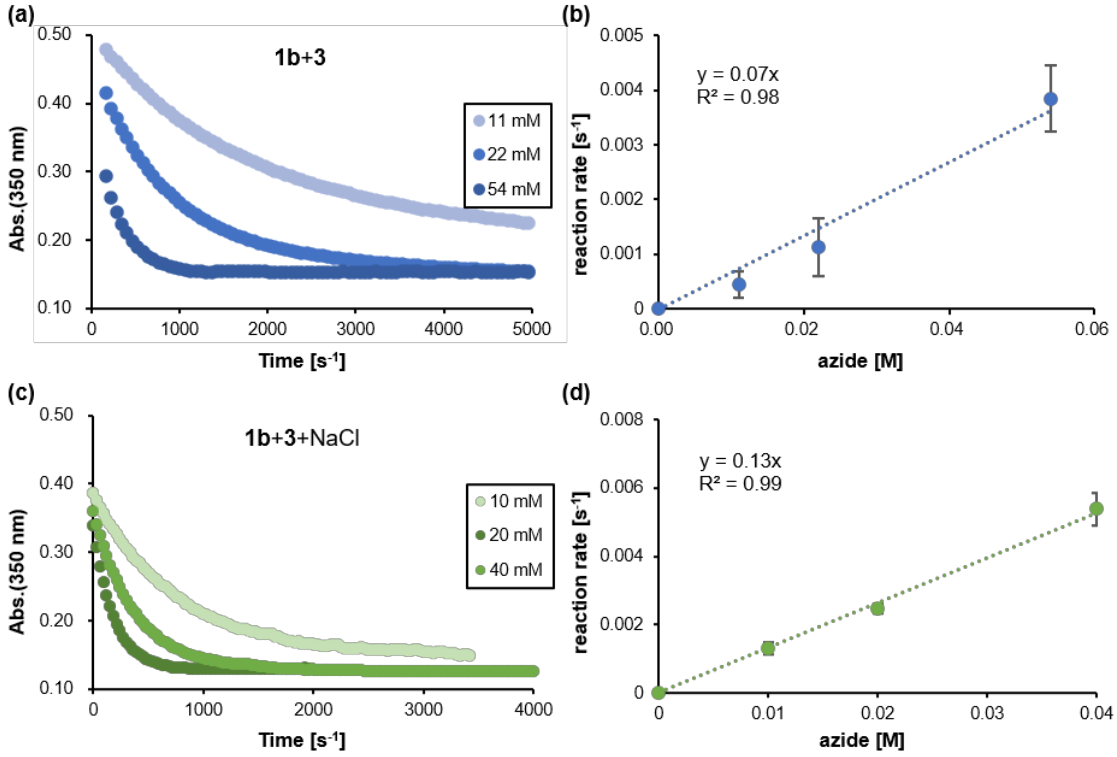

Fig. S4 (a) Normalized first-order exponential decay of DSP-CODY (**1b**) absorbance (350 nm) in the presence of **3** in H_2O at 25 ºC, monitored over time, where [**1b**] = 1.0 mM, and [**3**] = 11, 22 or 54 mM. (b) Linear regression of pseudo-first order rates versus **3** concentrations to derive the apparent second-order rate constant. (c) Normalized first-order exponential decay of **1b** absorbance (350 nm) in the presence of **3** and NaCl in H_2O at 25 ºC, monitored over time, where [**1b**] = 1.0 mM, [**3**] = 10, 20 or 40 mM, and [NaCl] = 100 mM. (d) Linear regression of pseudo-first order rates versus **3** concentrations in the presence of NaCl to derive the apparent second-order rate constant. Data represent the mean from three independent experiments and error bars show standard deviation (SD).

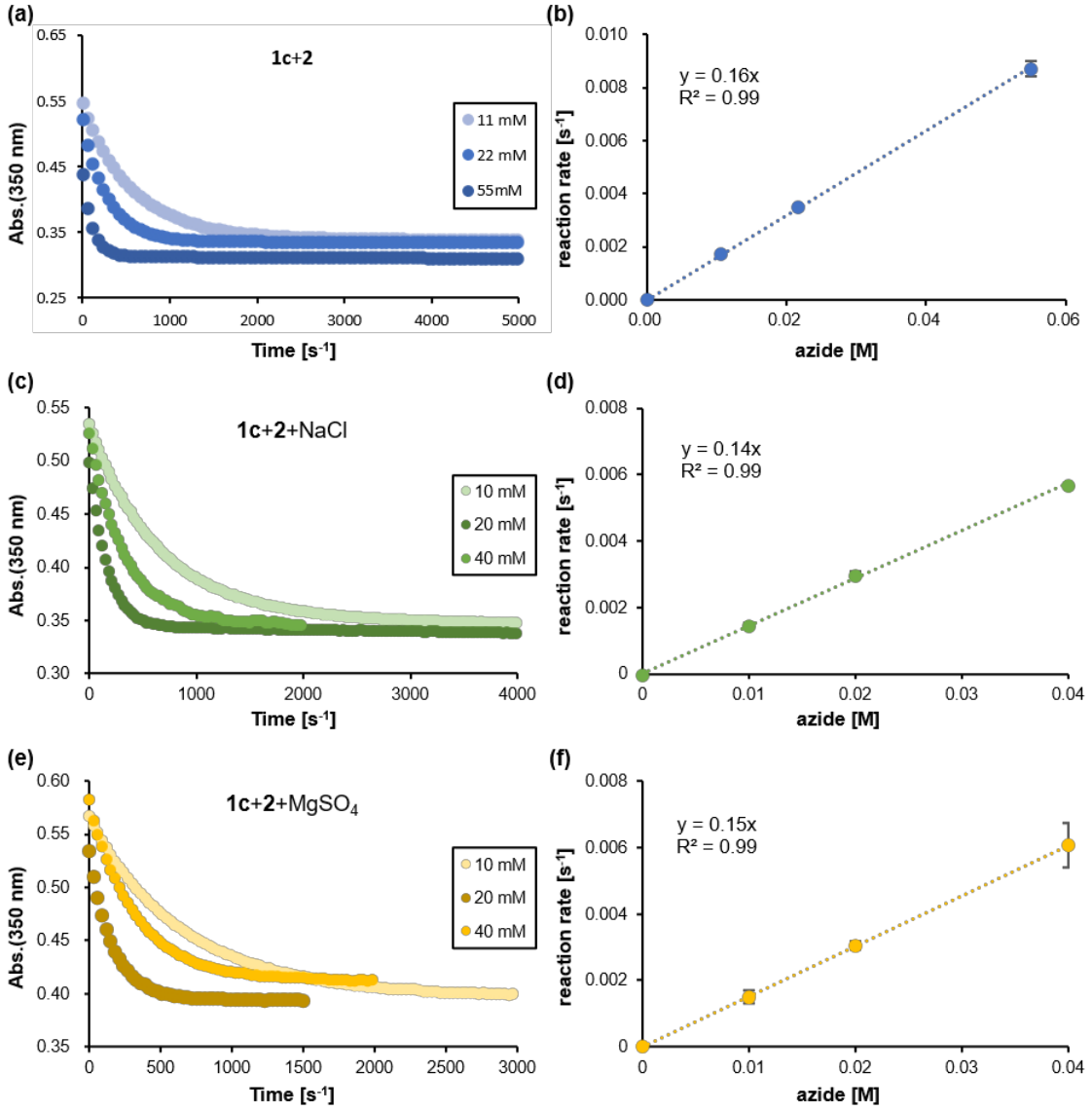

Fig. S5 (a) Normalized first-order exponential decay of DHTAU-CODY (**1c**) absorbance (350 nm) in the presence of **2** in H_2O at 25 ºC, monitored over time, where [**1c**] = 0.96 mM, and [**2**] = 11, 22 or 55 mM. (b) Linear regression of pseudo-first order rates versus **2** concentrations to derive the apparent second-order rate constant. (c) Normalized first-order exponential decay of **1c** absorbance (350 nm) in the presence of **2** and NaCl in H_2O at 25 ºC, monitored over time, where [**1c**] = 1.2 mM, [**2**] = 10, 20 or 40 mM, and [NaCl] = 100 mM. (d) Linear regression of pseudo-first order rates versus **2** concentrations in the presence of NaCl to derive the apparent second-order rate constant. (e) Normalized first-order exponential decay of **1c** absorbance (350 nm) in the presence of **2** and $MgSO_4$ in H_2O at 25 ºC, monitored over time, where [**1c**] = 1.2 mM, [**2**] = 10, 20 or 40 mM, and [$MgSO_4$] = 100 mM. (f) Linear regression of pseudo-first order rates versus **2** concentrations in the presence of $MgSO_4$ to derive the apparent second-order rate constant. Data represent the mean from three

independent experiments and error bars show standard deviation (SD).

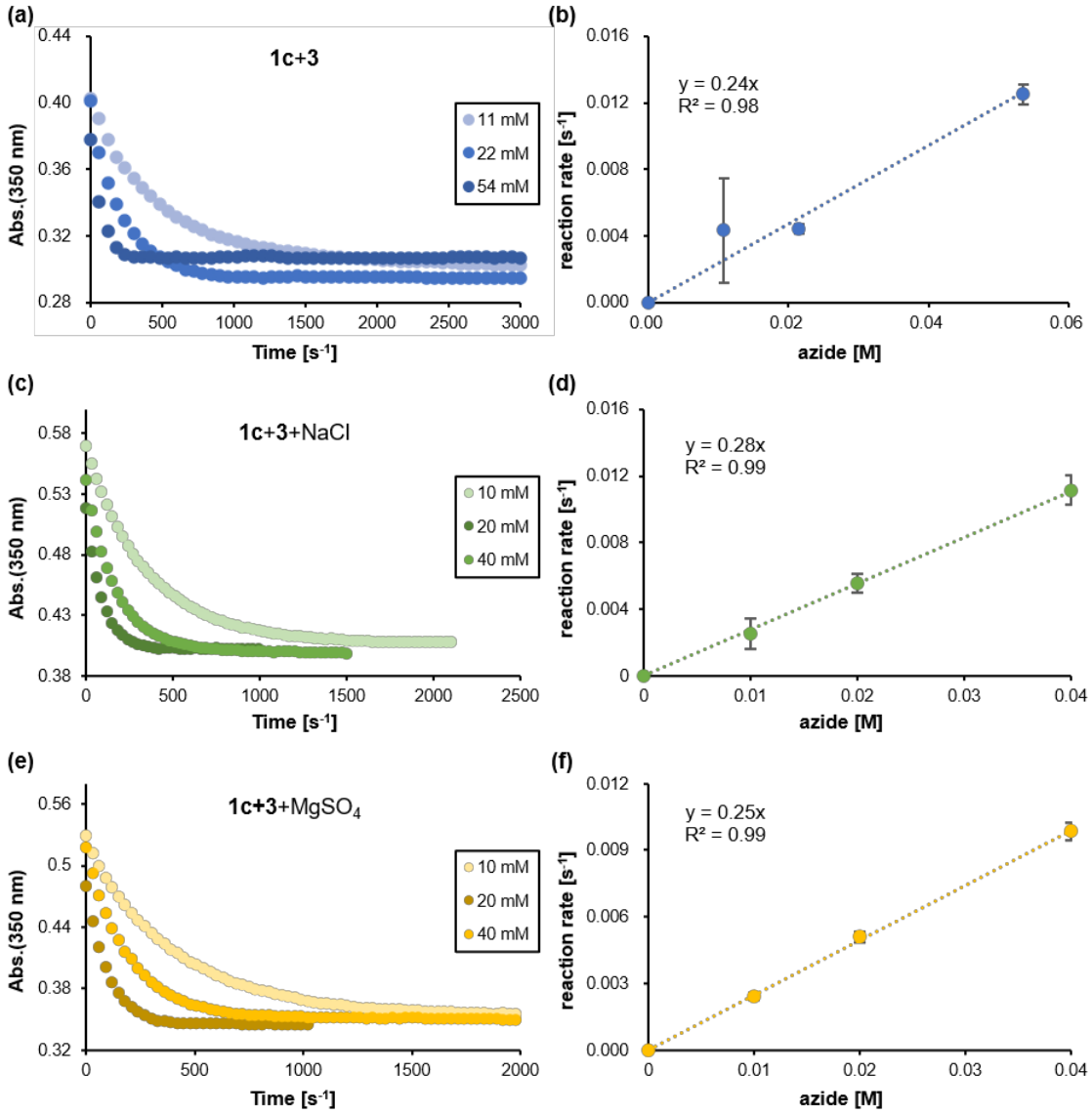

Fig. S6 (a) Normalized first-order exponential decay of DHTAU-CODY (**1c**) absorbance (350 nm) in the presence of **3** in H_2O at 25 ºC, monitored over time, where [**1c**] = 0.96 mM, and [**3**] = 11, 22 or 54 mM. (b) Linear regression of pseudo-first order rates versus **3** concentrations to derive the apparent second-order rate constant. (c) Normalized first-order exponential decay of **1c** absorbance (350 nm) in the presence of **3** and NaCl in H_2O at 25 ºC, monitored over time, where [**1c**] = 1.2 mM, [**3**] = 10, 20 or 40 mM, and [NaCl] = 100 mM. (d) Linear regression of pseudo-first order rates versus **3** concentrations in the presence of NaCl to derive the apparent second-order rate constant. (e) Normalized first-order exponential decay of **1c** absorbance (350 nm) in the presence of **3** and $MgSO_4$ in H_2O at 25 ºC, monitored over time, where [**1c**] = 1.2 mM, [**3**] = 10, 20 or 40 mM, and [$MgSO_4$] = 100 mM. (f) Linear regression of pseudo-first order rates versus **3** concentrations in the presence of

$MgSO_4$ to derive the apparent second-order rate constant. Data represent the mean from three independent experiments and error bars show standard deviation (SD).

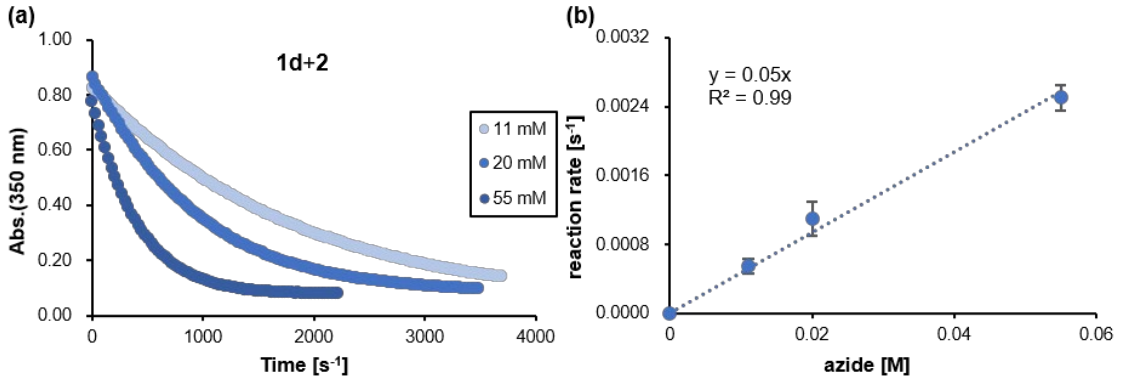

Fig. S7 (a) Normalized first-order exponential decay of CODY (**1d**) absorbance (350 nm) in the presence of **2** in MeOH at 25 ºC, monitored over time, where [**1d**] = 1.0 mM, and [**2**] = 11, 20 or 55 mM. (b) Linear regression of pseudo-first order rates versus **2** concentrations to derive the apparent second-order rate constant.

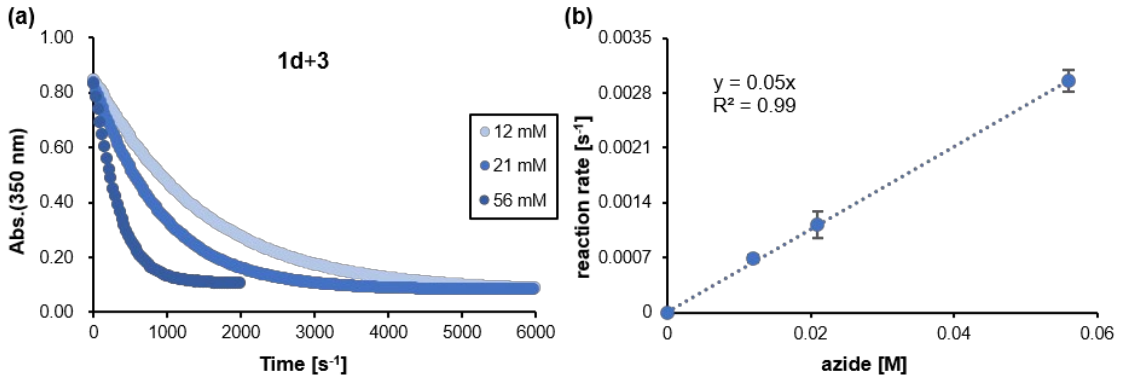

Fig. S8 (a) Normalized first-order exponential decay of CODY (**1d**) absorbance (350 nm) in the presence of **3** in MeOH at 25 ºC, monitored over time, where [**1d**] = 1.0 mM, and [**3**] = 12, 21 or 56 mM. (b) Linear regression of pseudo-first order rates versus **3** concentrations to derive the apparent second-order rate constant.

3. Regioselectivity analysis of the reaction between DMA-CODY (1a) and sodium 3-azidopropane-1-sulfonate (3) by HPLC and NMR.

1a (7.6 mM) was reacted with **3** (15.2 mM) in H_2O for 24 h. The mixture was analyzed by reversed-phase HPLC. Conditions of reversed-phase HPLC: Column, YMC-Triart C18, 20×250mm; Mobile phase A, 0.1% TFA in H_2O; B, 0.1% TFA in CH_3CN; Isocratic elution, A: 90%, B: 10%; Flow rate at 4.5 mL/min; UV detection at 254 nm.

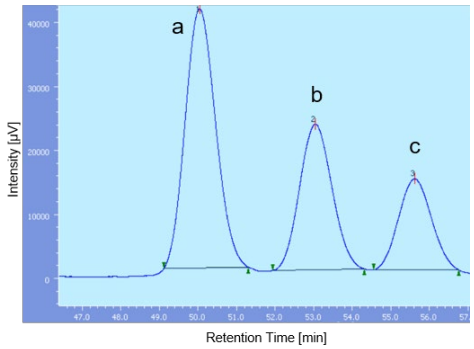

No.	Retention Time	Area	Area [%]	Height
a	50.038	2218680	50.586	40400
b	53.035	1326428	30.242	22712
c	55.608	840891	19.172	14216

Fig. S9 Reverse phase HPLC analysis of the click reaction products between **1a** and **3.**

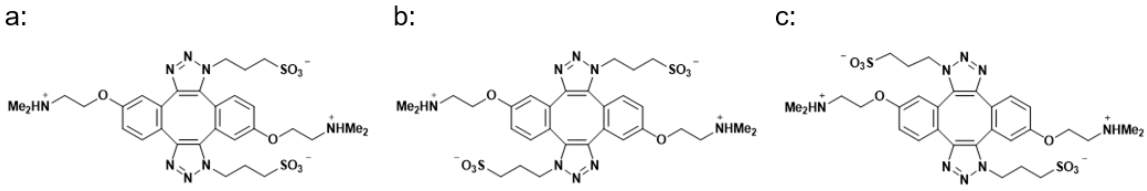

Fig. S10 Structure of a-c determined by ROESY.

5a

^{1}H-NMR (800 MHz, CD_3OD) δ 7.53 (d, J=8.33 Hz, 1H, H7'), 7.50 (d, J=8.69 Hz, 1H, H7), 7.30 (dd, J=2.33, 8.66 Hz, 1H, H8), 7.25 (s, 1H, H9), 7.21 (s, 1H, H9'), 7.20 (d, J=2.66 Hz, 1H, H8'), 4.69 (m, 1H, H1b'), 4.58 (m, 2H, H4b, H1b), 4.50 (m, 2H, H1a', H1a), 4.44 (m, 3H, H4a, H4a'), 3.61 (m, 4H, H5, H5'), 3.00 (m, 7H, H6, H3b', H6'), 2.91 (m, 1H, H3a'), 2.80 (m, 1H, , H3b), 2.71 (s, 1H, , H3a), 2.50 (m, 2H, , H2b', H2a'), 2.32 (m, 2H,H2); ^{13}C-NMR (200 MHz, CD_3OD) δ 160.448, 159.7403, 146.2488, 145.981, 135.4512, 135.1795, 133.734, 133.71, 132.9388, 130.3661, 125.6278, 121.4026, 118.7497, 118.178, 117.1783, 116.785, 63.5217, 63.3283, 57.6442, 57.6107, 49.1259, 48.8814, 48.558, 43.9895, 43.8927, 26.7994; HRMS (ESI-TOF) 705.2466 $(M + H)^+$ calcd for $C_{30}H_{40}N_8O_8S_2H$ 705.2483.

5b

^{1}H-NMR (800 MHz, CD_3OD) δ 7.46 (d, J=8.51 Hz, 1H, H7), 7.28 (s, 1H, H9), 7.27 (d, J=8.55 Hz,1H, H8), 4.57 (m, 1H, H1b), 4.47 (t, J=4.73 Hz, 2H, H4), 4.37 (m, 1H, H1a), 3.64 (m, 2H, H5), 2.83 (s, 3H, H6), 2.74 (m, 1H, H3b), 2.70 (m, 1H, H3a), 2.24 (m, 2H, H2); ^{13}C-NMR (200 MHz, CD_3OD) δ 160.4108, 145.7033, 135.8823, 135.0766, 133.1027, 120.463, 117.7695, 117.5319, 63.4078, 57.5221, 49.1648, 47.9464, 43.9268, 30.7501; HRMS (ESI-TOF) 705.2482 $(M + H)^+$ calcd for $C_{30}H_{40}N_8O_8S_2H$ 705.2483.

5c

^{1}H-NMR (800 MHz, CD_3OD) δ 7.58 (d, J=8.63 Hz, 1H, H7), 7.25 (dd, J=2.60, 8.63 Hz, 1H, H8), 7.17 (d, J=2.58 Hz, 1H, H9), 4.67 (m, 1H, H1b), 4.60 (m, 1H, H4b), 4.39 (m, 2H, H4a), 3.61 (m, 2H, H5), 3.02 (m, 7H, H6a, H3b, H6b), 2.90 (m, 1H, H3a), 2.49 (m, 1H, H2b), 2.43 (m, 1H, H2a); ^{13}C-NMR (200 MHz, CD_3OD) δ 159.8012, 145.4102, 135.7351, 133.5467, 128.8287, 126.3309, 117.7645, 117.6612, 63.3204, 57.8461, 49.1624, 48.4284, 44.4593, 43.8099, 26.8893; HRMS (ESI-TOF) 705.25 $(M + H)^+$ calcd for $C_{30}H_{40}N_8O_8S_2H$ 705.2483.

4. Synthesis of azide modified protein.

Lysozyme (100 ng, 10 mg/ml in 1× PBS, pH 7.4) was incubated with azide NHS ester (**S1**) (8.8 µL of 0.4 mM in DMSO, 0.5 eq to the mol number of lysozyme) in a final volume of 200 µL of 1×PBS at room temperature for 2 h. Similarly, HSA (100 ng, 10 mg/ml in 1× PBS, pH 7.4) was incubated with azide NHS ester (**S1**) (8.8 µL of 0.09 mM in DMSO, 0.5 eq to the mol number of HSA) in a final volume of 200 µL of 1×PBS at room temperature for 2 h. Orosomucoid (100 ng, 10 mg/ml in 0.1 M HEPES, pH 8.1) azide NHS ester (**S1**) (8.8 µL of 0.09 mM in DMSO, 0.5 eq to the mol number of orosomucoid) in a final volume of 200 µL of 1×PBS at room temperature for 2 h. The reaction was quenched by adding 5 µL of 100mM Tris-HCl (pH 7.5) to the mixture. Residual NHS ester # were removed by dialysis against 1× PBS using Amicon centrifugal filter units (10 kDa MWCO). Protein concentrations were determined by the Bradford protein assay.

By analyzing LC/MS/MS, lysozyme was calculated that about 3 lysine groups were modified, and 3 2 lysine groups of HSA were modified (Fig.S10, S12-16). Identifying the site of modification of orosomucoid was difficult due to complex glycosylation.

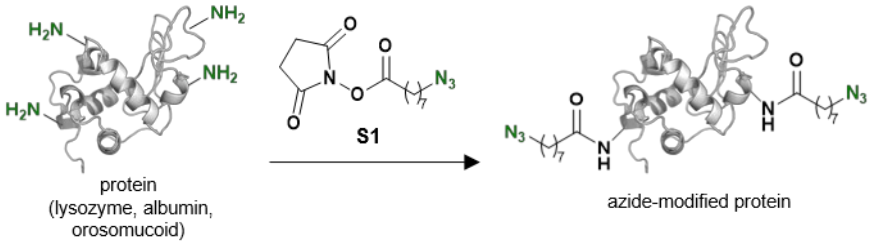

Fig. S11 Schematic illustration of azido modification.

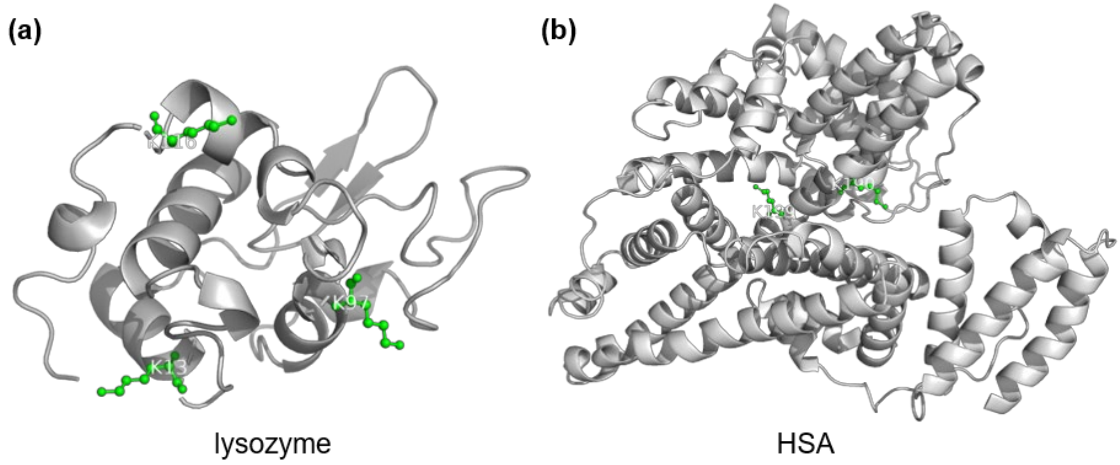

Fig. S12 Azido-modified lysine residues of (a) lysozyme and (b) HSA.

5. Protein labeling.

Azide modified protein (LYS, ORM, 6 μM for (a) and (b), 1–0.0625 μM for (c)) was reacted with **1a** or **1b** (100 μM for (a) and (b), 10 μM for (c)) for 0-120 sec (for (a) and (b), 60 sec for (c)) followed by Flu-N_3 (**4**, 100 μM for (a) and (b), 10 μM for (c)) for 30 min in 1× PBS (pH 7.4) at 4 °C and the reaction was quenched with 1 μL of 2-azidoethanol (**2**). The reaction products were analyzed by SDS-PAGE on 10% (for HSA and orosomucoid) and 15% (for lysozyme) polyacrylamide gels. Protein staining was performed according to standard protocols using Coomassie Brilliant Blue G250.

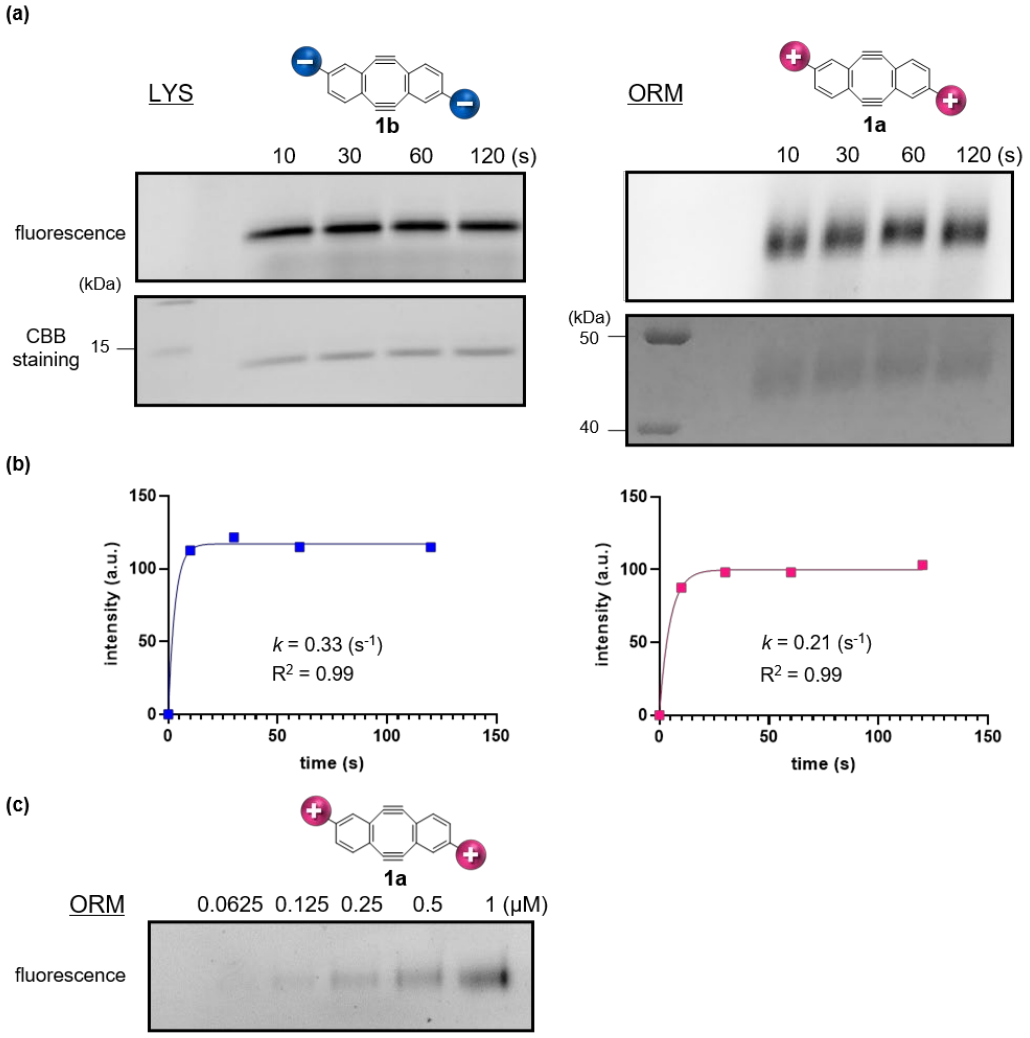

Fig. S13 (a) SDS-PAGE analyses of the time course of fluorescence labelling during the reaction of lysozyme with WS-CODY (**1b**) and Flu-N_3, and orosomucoid with WS-CODY (**1a**) and Flu-N_3. proteins were visualized with Coomassie brilliant blue staining. (b) Analysis of first-order kinetics of labelling using the band intensities quantified by Image J. Data were fitted by non-linear regression. (c) SDS-PAGE analyses of the reaction of various concentrations of orosomucoid (0.0625–1 μM) with WS-CODY (**1a**) (10 μM) and Flu-N_3 (10 μM).

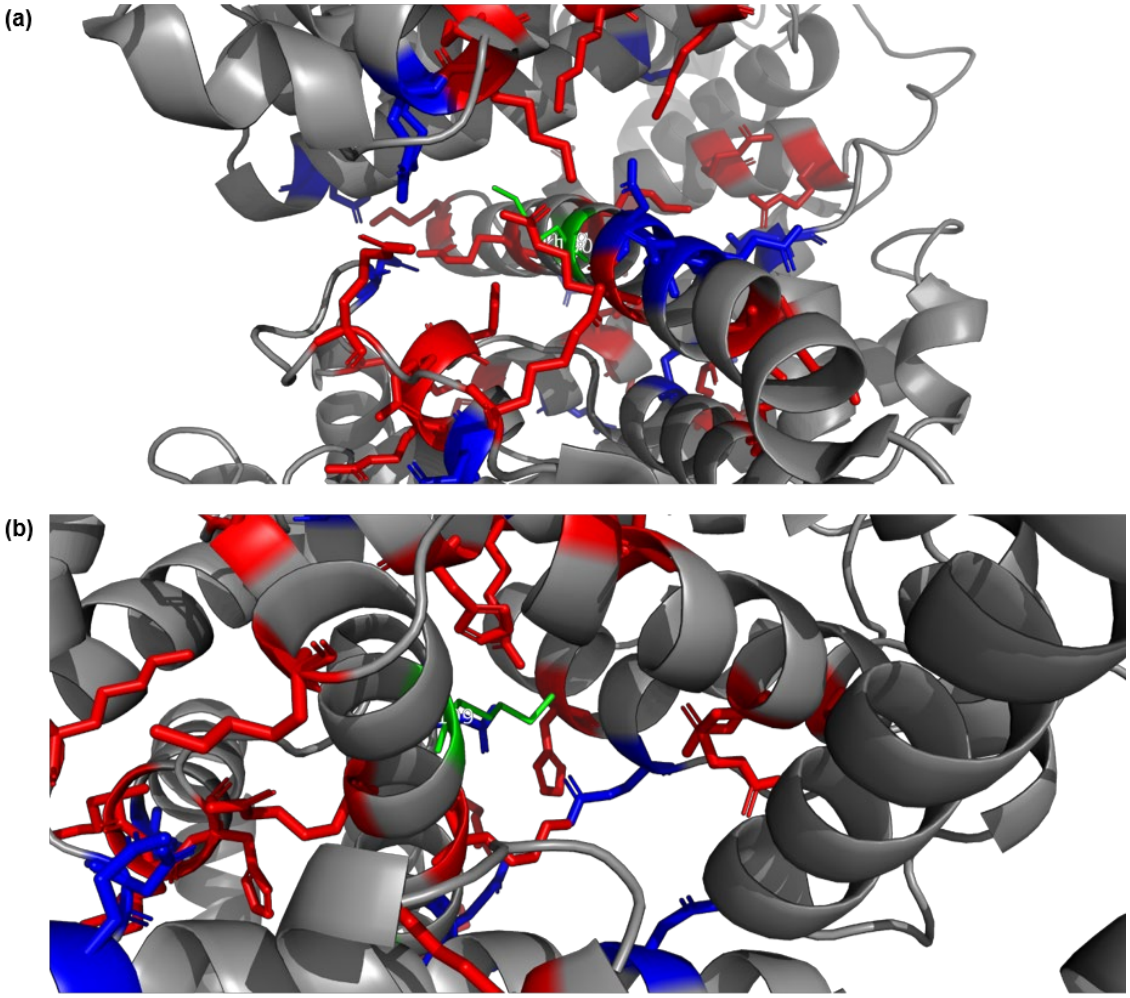

Fig. S14 Amino acids around the azide-modified sites (a) K190 and (b) K199 of HSA. Acidic amino acids (aspartic acid, glutamic acid) showed in blue (16 residues), basic amino acids (lysine, arginine, histidine) showed in red (29 residues), and azide-modified sites (K190, K199) showed in green.

6. LC/MS/MS analysis.

SP3 protocol was used to perform protein digestion.[1] Briefly, To a solution of 10 µg of azide modified and unmodified protein (lysozyme and HSA) in PBS (10 µL), 30 µL of 100mM Tris-HCl pH8.5, 2 % SDS and 4 µL of 100 mM DTT was added ,and then incubated at 50 °C for 30 min. Next, reduced disulfides were alkylated by adding 4 µL of 360 mM IAA, and incubated at room temperature in the dark for 30 min. 20 µL suspension of SP3 beads added to the samples and 170 µL ethanol was added to induce binding of the proteins to the beads. After a 10 min incubation at room temperature with shaking, beads were washed with 800 µL of 80% ethanol three times and 800 µL of acetonitrile. After air-dry the SP3 beads, 100 µL of 50 mM Tris-HCl pH8.0 was added and sonicated 5 min (five times every 30 s) to fully disaggregate the beads. Next, proteins were digested by adding 1 µL of 500 ng/µL LysC/trypsin (Promega) at 37 °C overnight. The reaction was quenched with 20 µL of 5% TFA and sonicated for 5 min. Samples were desalted with GL-Tip SDB (GL sciences) according to the manufacturer's instructions and dried them under vacuum. Samples were dissolved in 40 µL of 2% acetonitrile (0.1% TFA) and were analyzed with LC/MS/MS.

mobile phase A: 0.1% formic acid in H_2O and mobile phase B: 0.1% formic acid in acetonitrile.

Analysis was performed using MS-DIAL 5.0.0.

Lysozyme (PDB:2cds)

KVFGRCELAAAMKRHGLDNYRGYSLGNWVCAAKFESNFNTQATNRNTDGSTDYGILQINS
RWWCNDGRTPGSRNLCNIPCSALLSSDITASVNCAKKIVSDGNGMNAWVAWRNRCKGTDV
QAWIRGCRL

HSA (PDB:1ao6)

DAHKSEVAHRFKDLGEENFKALVLIAFAQYLQQCPFEDHVKLVNEVTEFAKTCVADESAEN
CDKSLHTLFGDKLCTVATLRETYGEMADCCAKQEPERNECFLQHKDDNPNLPRLVRPEVDV
MCTAFHDNEETFLKKYLYEIARRHPYFYAPELLFFAKRYKAAFTECCQAADKAACLLPKLDE
LRDEGKASSAKQRLKCASLQKFGERAFKAWAVARLSQRFPKAEFAEVSKLVTDLTKVHTEC
CHGDLLECADDRADLAKYICENQDSISSKLKECCEKPLLEKSHCIAEVENDEMPADLPSLAA
DFVESKDVCKNYAEAKDVFLGMFLYEYARRHPDYSVVLLLRLAKTYETTLEKCCAAADPH
ECYAKVFDEFKPLVEEPQNLIKQNCELFEQLGEYKFQNALLVRYTKKVPQVSTPTLVEVSRN
LGKVGSKCCKHPEAKRMPCAEDYLSVVLNQLCVLHEKTPVSDRVTKCCTESLVNRRPCFSA
LEVDETYVPKEFNAETFTFHADICTLSEKERQIKKQTALVELVKHKPKATKEQLKAVMDDFA
AFVEKCCKADDKETCFAEEGKKLVAASQAALGL

Lysozyme_K13: CELAAAMKR

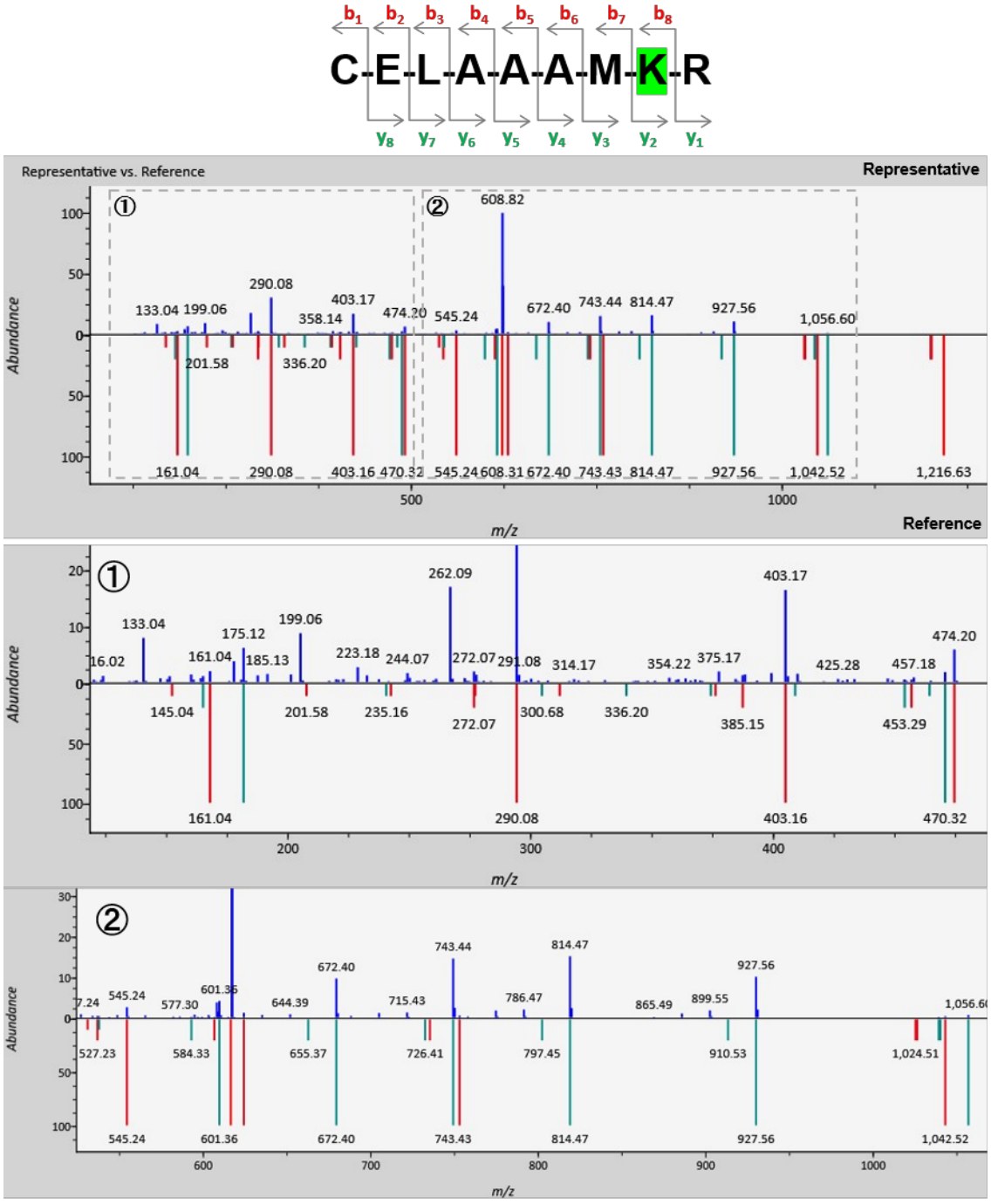

Fig. S15 Spectrum of fragment (CELAAAMKR).

Table.S1 Expected b and y ions (ions that are found are highlighted in red and green).

Residue	b#	b	y	y#
C (Carbamidomethyl)	1	161.04	-	
E	2	290.08	1056.60	8
L	3	403.17	927.56	7
A	4	474.20	814.47	6
A	5	545.24	743.44	5
A	6	616.28	672.40	4
M	7	747.32	601.36	3
K	8	1042.51	470.32	2
R		-	175.12	1

Lysozyme_K97: KIVSDGNGMNAWVAWR

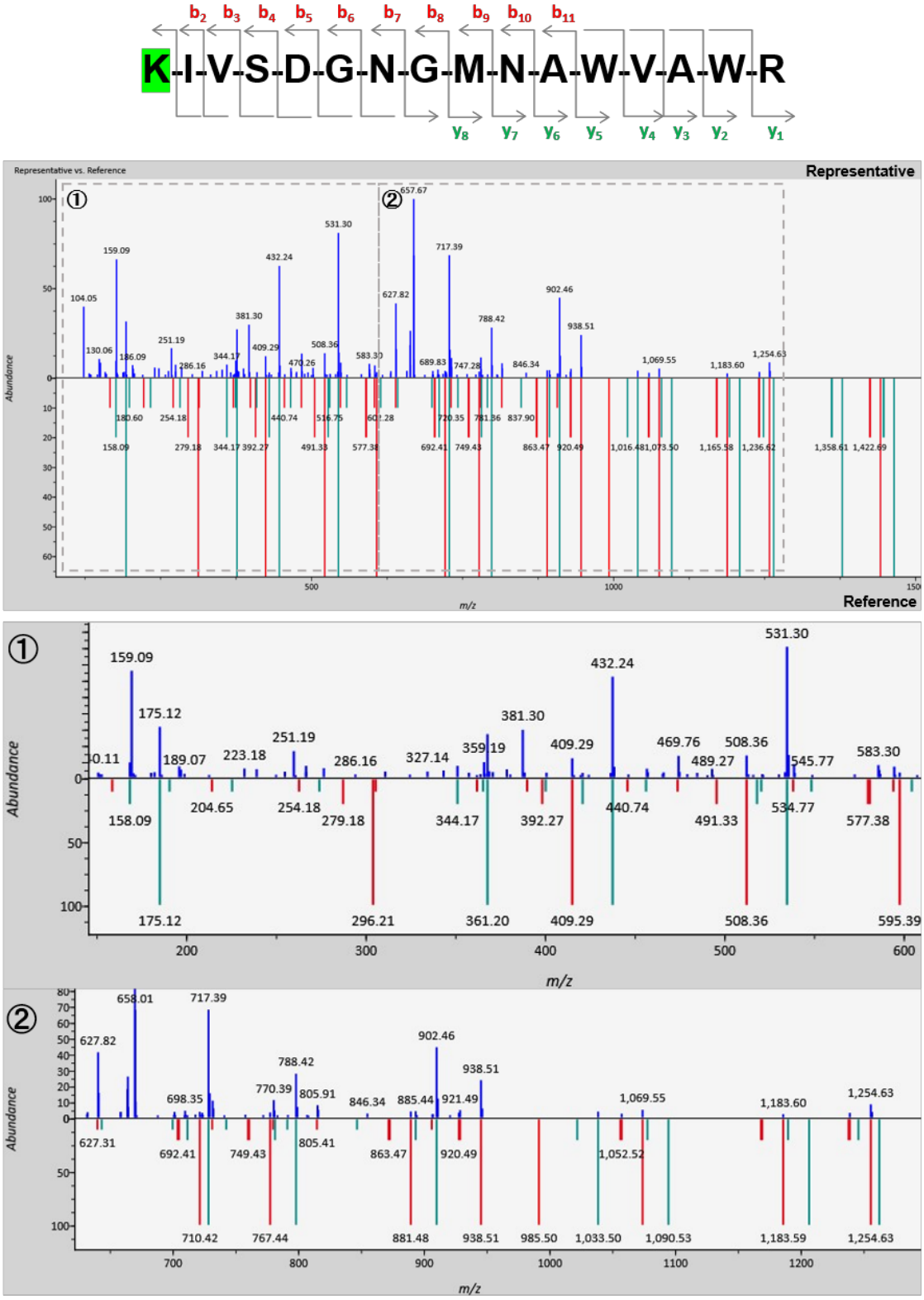

Fig. S16 Spectrum of fragment (KIVSDGNGMNAWVAWR).

Table.S2 Expected b and y ions (ions that are found are highlighted in red and green).

Residue	b#	b	y	y#
K	1	296.21	-	
I	2	409.29	-	
V	3	508.36	-	
S	4	595.39	1463.65	13
D	5	710.42	1376.62	12
G	6	767.44	1261.59	11
N	7	881.49	1204.57	10
G	8	938.51	1090.53	9
M	9	1069.55	1033.50	8
N	10	1183.60	902.46	7
A	11	1254.63	788.42	6
W	12	1440.71	717.38	5
V		-	531.30	4
A		-	432.24	3
W		-	361.20	2
R		-	175.12	1

Lysozyme_K116: CKGTDVQAWIR

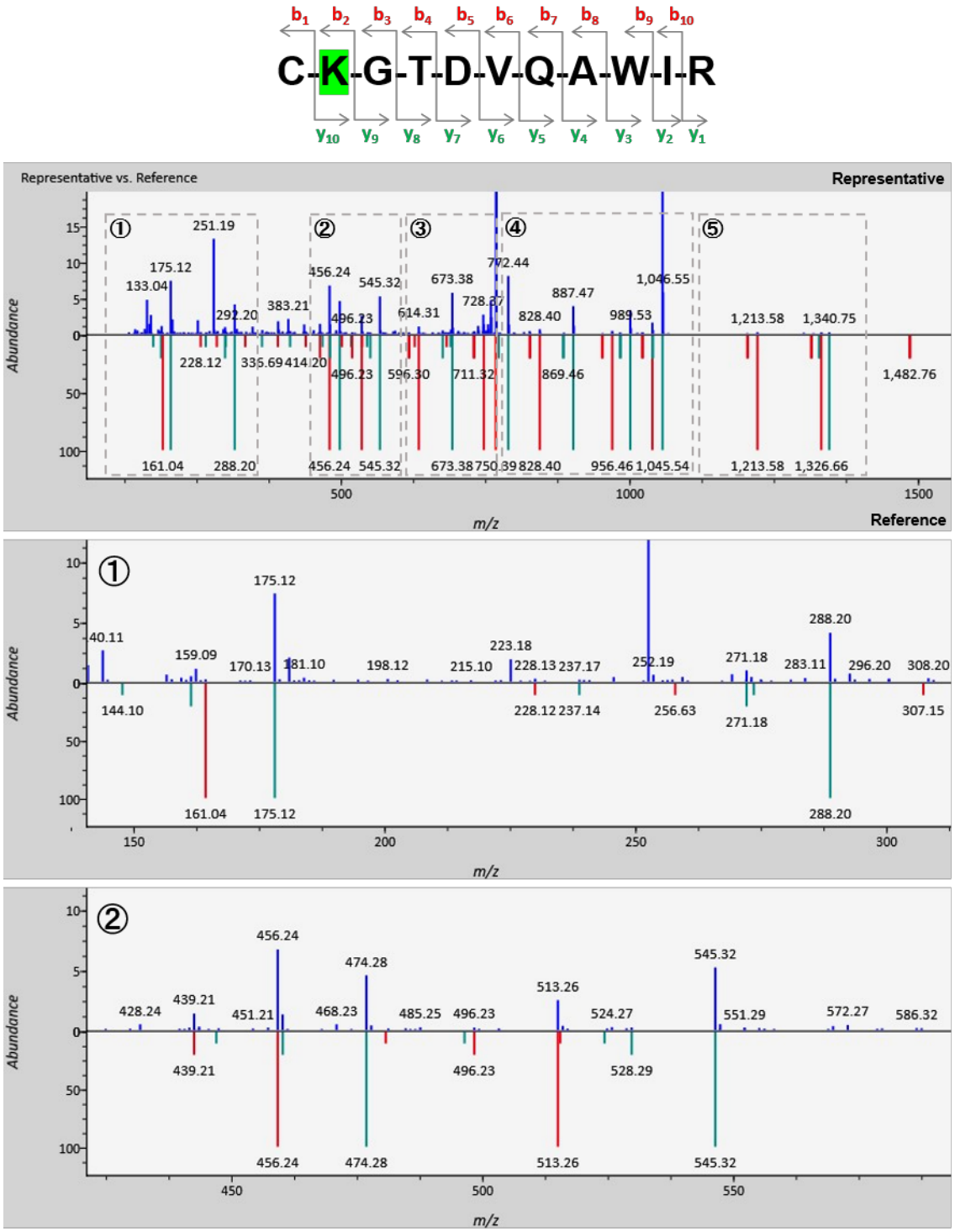

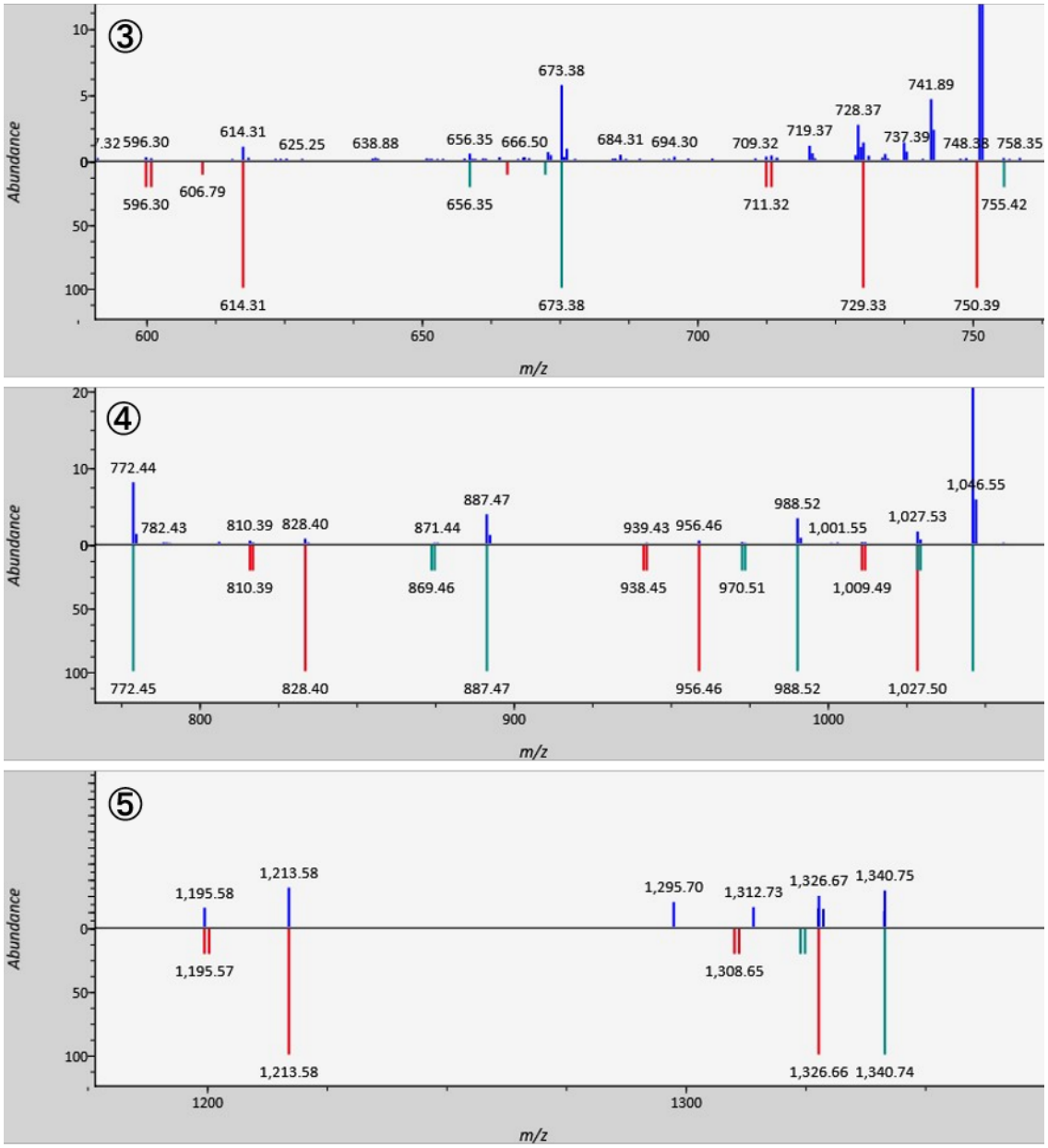

Fig. S17 Spectrum of fragment (CKGTDVQAWIR)**.**

Table.S3 Expected b and y ions (ions that are found are highlighted in red and green).

Residue	b#	b	y	y#
C (Carbamidomethyl)	1	161.04	-	
K	2	456.24	1340.75	10
G	3	513.26	1045.54	9
T	4	614.31	988.52	8
D	5	729.33	887.47	7
V	6	828.40	772.45	6
Q	7	956.46	673.38	5
A	8	1027.53	545.32	4
W	9	1213.58	474.28	3
I	10	1326.66	288.20	2
R		-	175.12	1

HSA_K190: LDELRDEGKASSAK

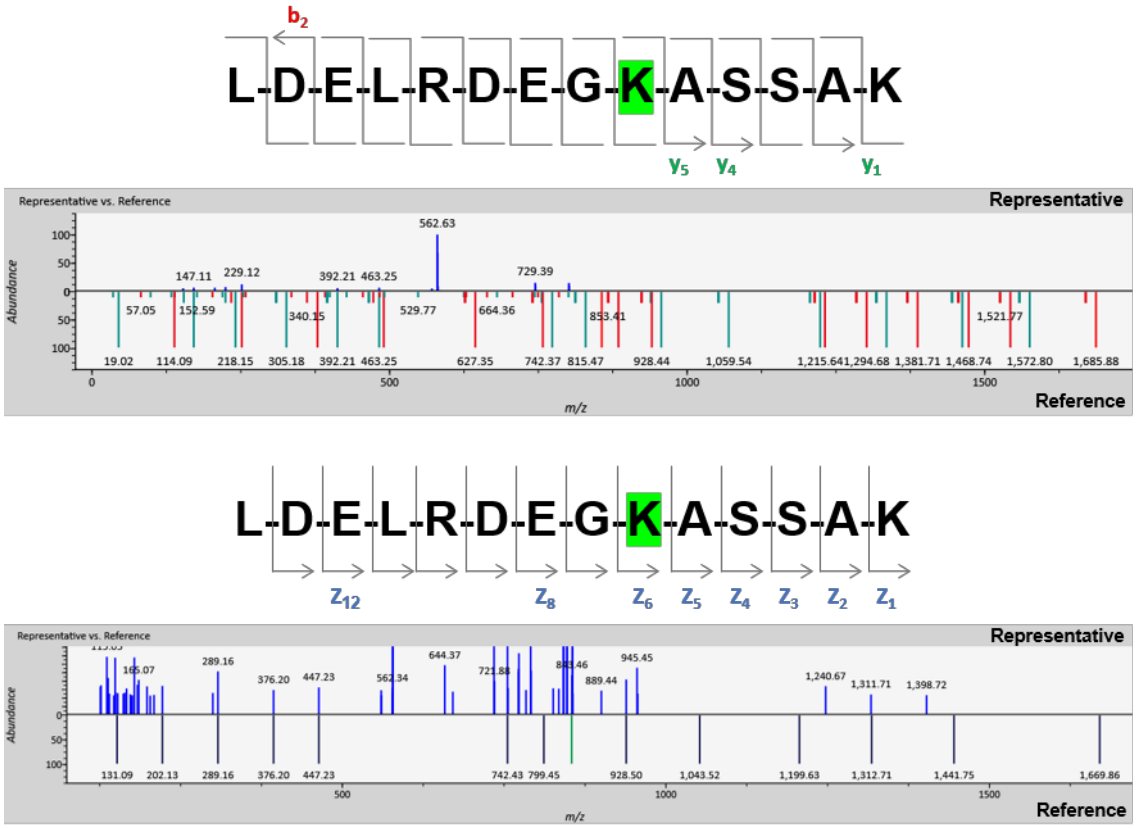

Fig. S18 Spectrum of fragment (LDELRDEGKASSAK).

Table.S4 Expected b, y, and z ions (ions that are found are highlighted in red, green, and blue).

Residue	b#	b	y	y#	z#	z
L	1	114.09	-			-
D	2	229.12	-	13	13	1669.86
E	3	358.16	1457.77	12	12	1441.75
L	4	471.24	1328.73	11	11	1311.71
R	5	627.35	1215.64	10	10	1199.63
D	6	742.37	1059.54	9	9	1043.52
E	7	871.42	944.52	8	8	928.50
G	8	928.44	815.47	7	7	799.45
K	9	1223.64	758.45	6	6	742.43
A	10	1294.68	463.25	5	5	447.23
S	11	1381.71	392.23	4	4	376.20
S	12	1468.74	305.18	3	3	289.16
A	13	-	218.15	2	2	202.13
K		-	147.11	1	1	131.19

K199: LKCASLQK

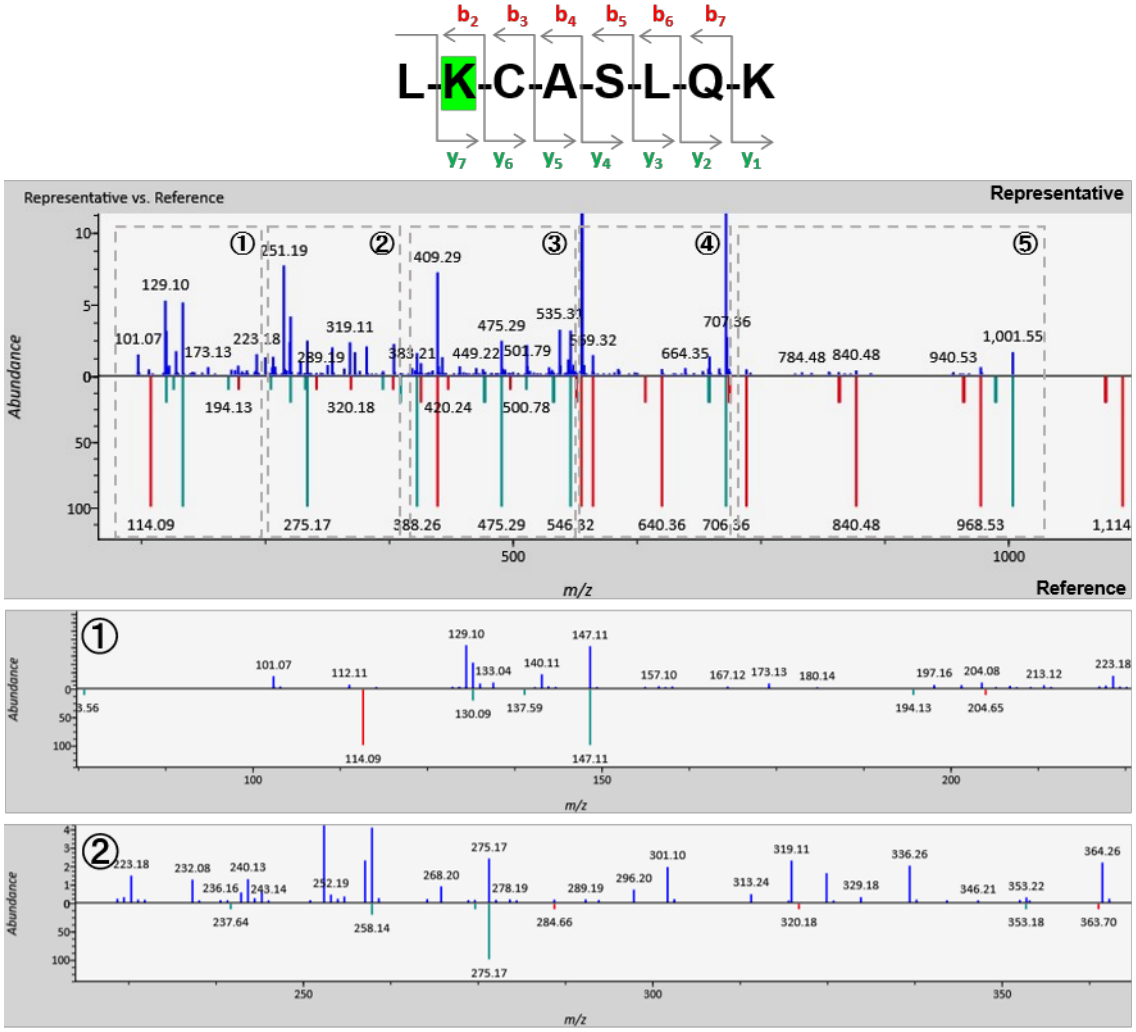

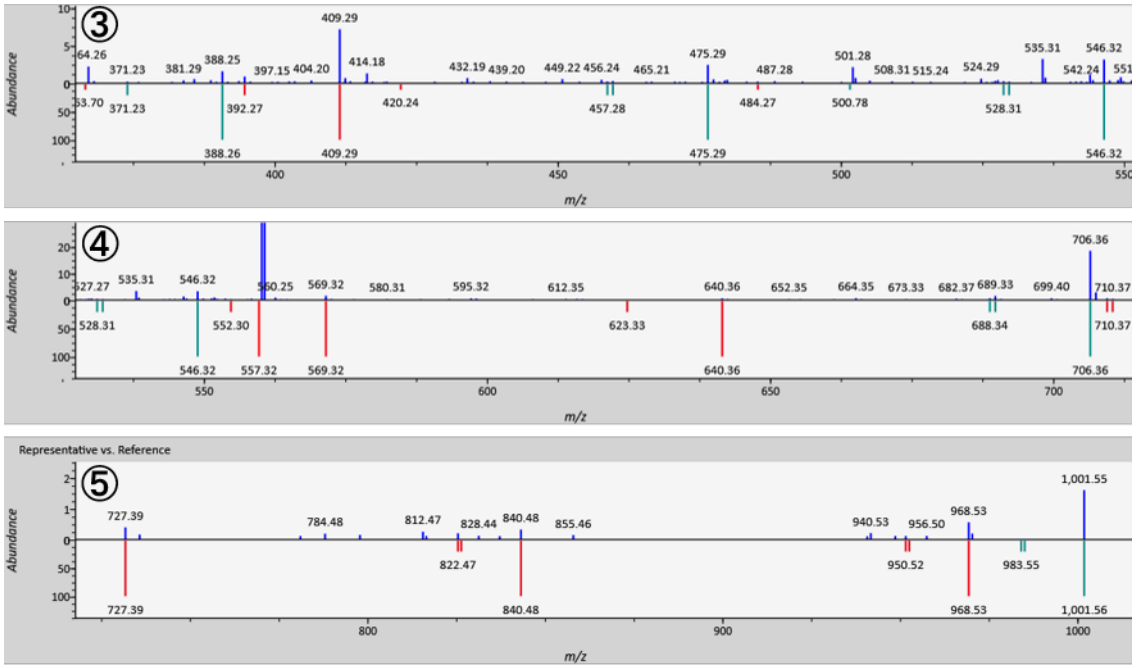

Fig. S19 Spectrum of fragment (LKCASLQK).

Table.S5 Expected b and y ions (ions that are found are highlighted in red and green).

Residue	b#	b	y	y#
L	1	114.09		
K	2	409.29	1001.56	7
C (Carbamidomethyl)	3	569.32	706.36	6
A	4	640.36	546.32	5
S	5	727.39	475.29	4
L	6	840.48	388.25	3
Q	7	968.53	275.17	2
K			147.11	1

7. Supplementary References

1 C. S. Hughes, S. Moggridge, T. Müller, P. H. Sorensen, G. B. Morin and J. Krijgsveld, *Nat. Protoc.*, 2019, **14**, 68–85.

8. ^{1}H and ^{13}C NMR Spectra

^{1}H NMR spectrum of **5a**.

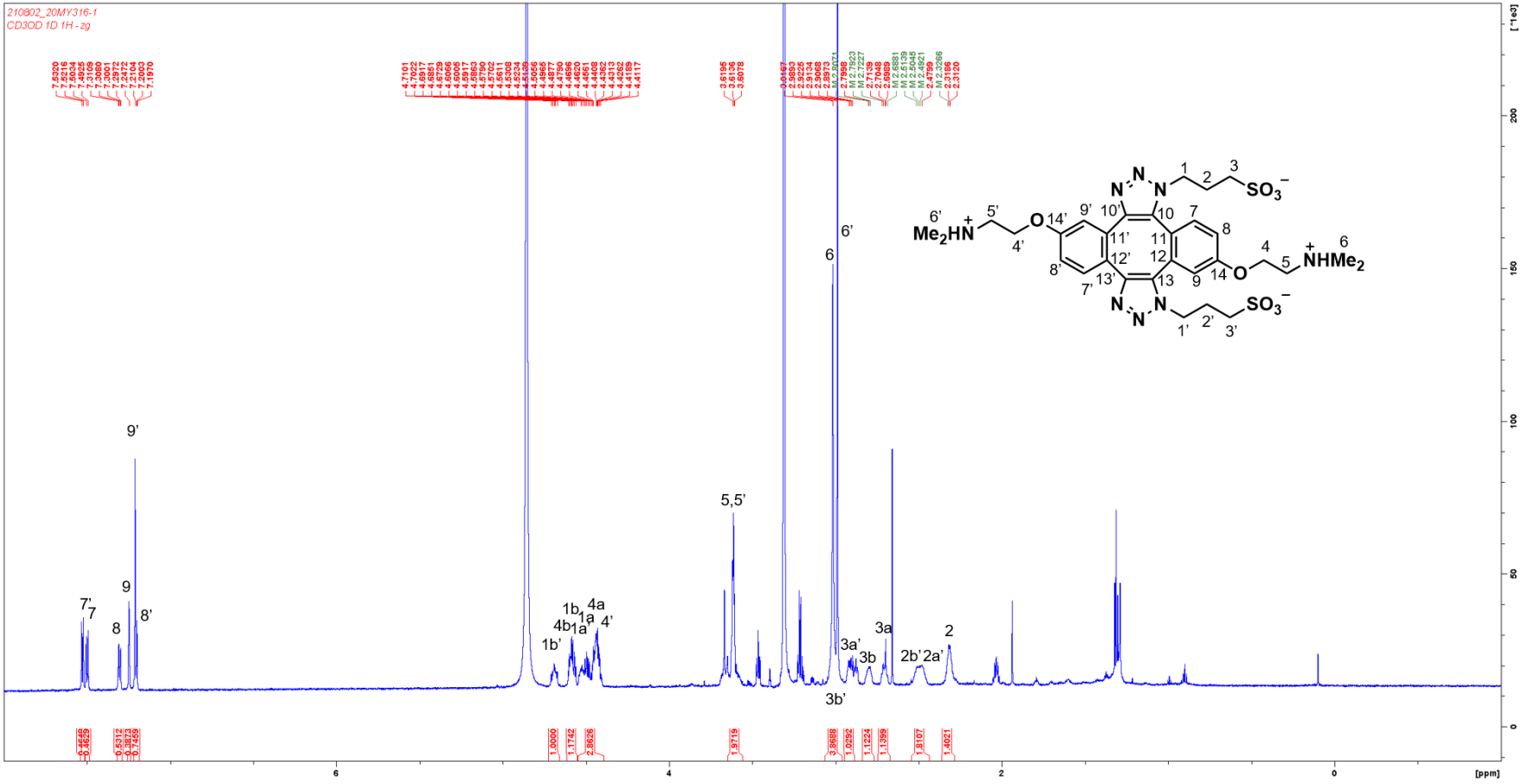

^{13}C NMR spectrum of **5a**.

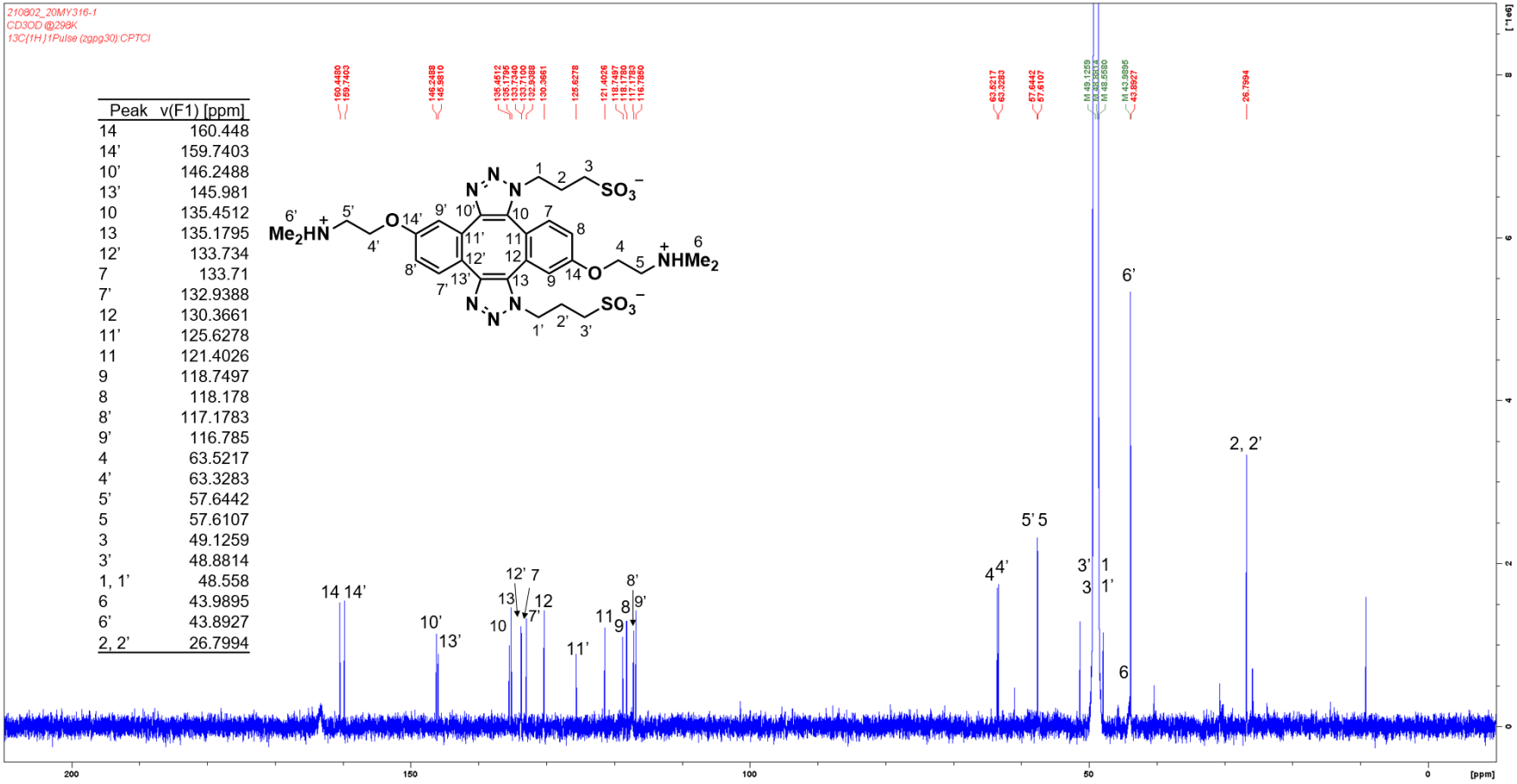

COSY spectrum of **5a**.

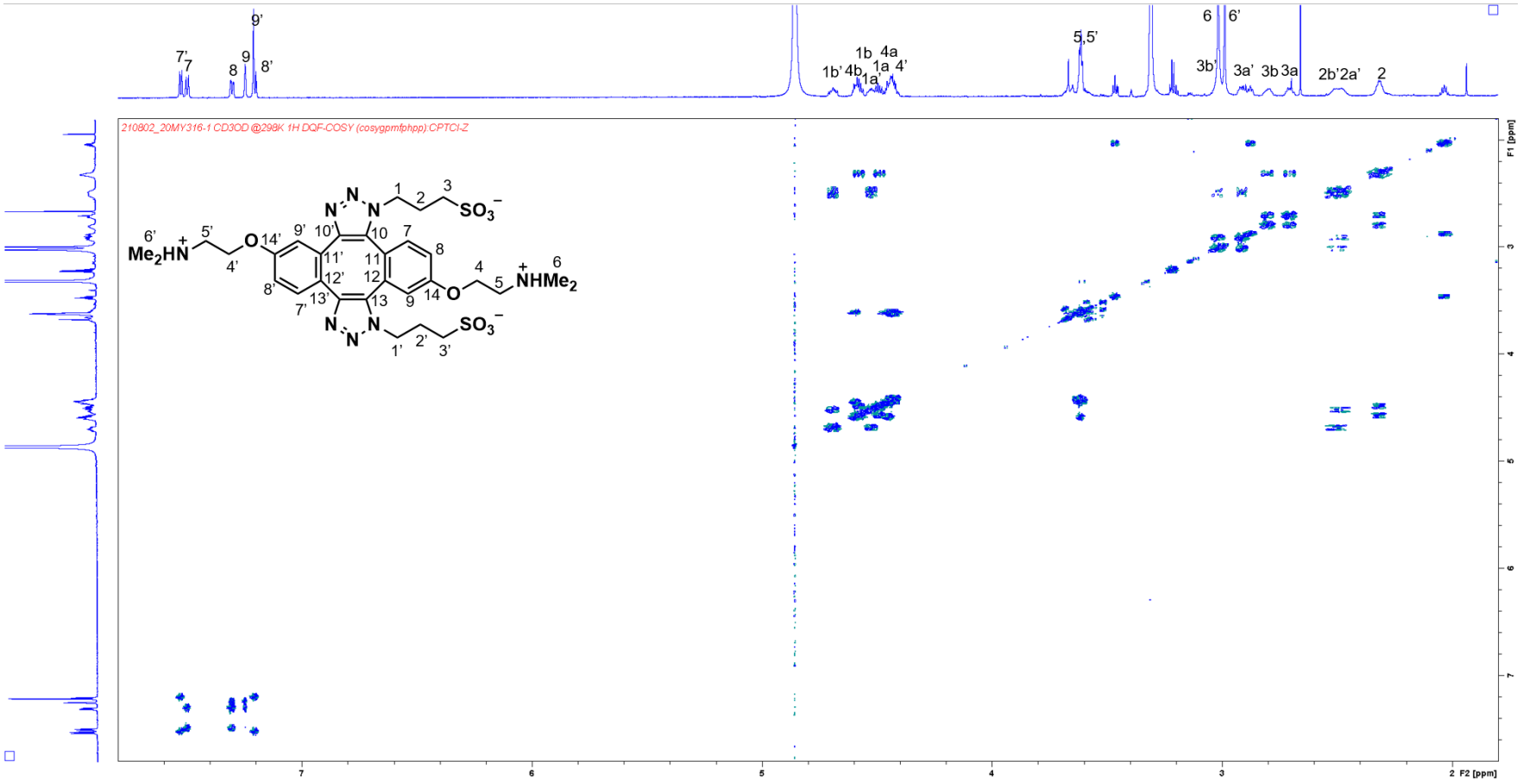

COSY spectrum of **5a**.

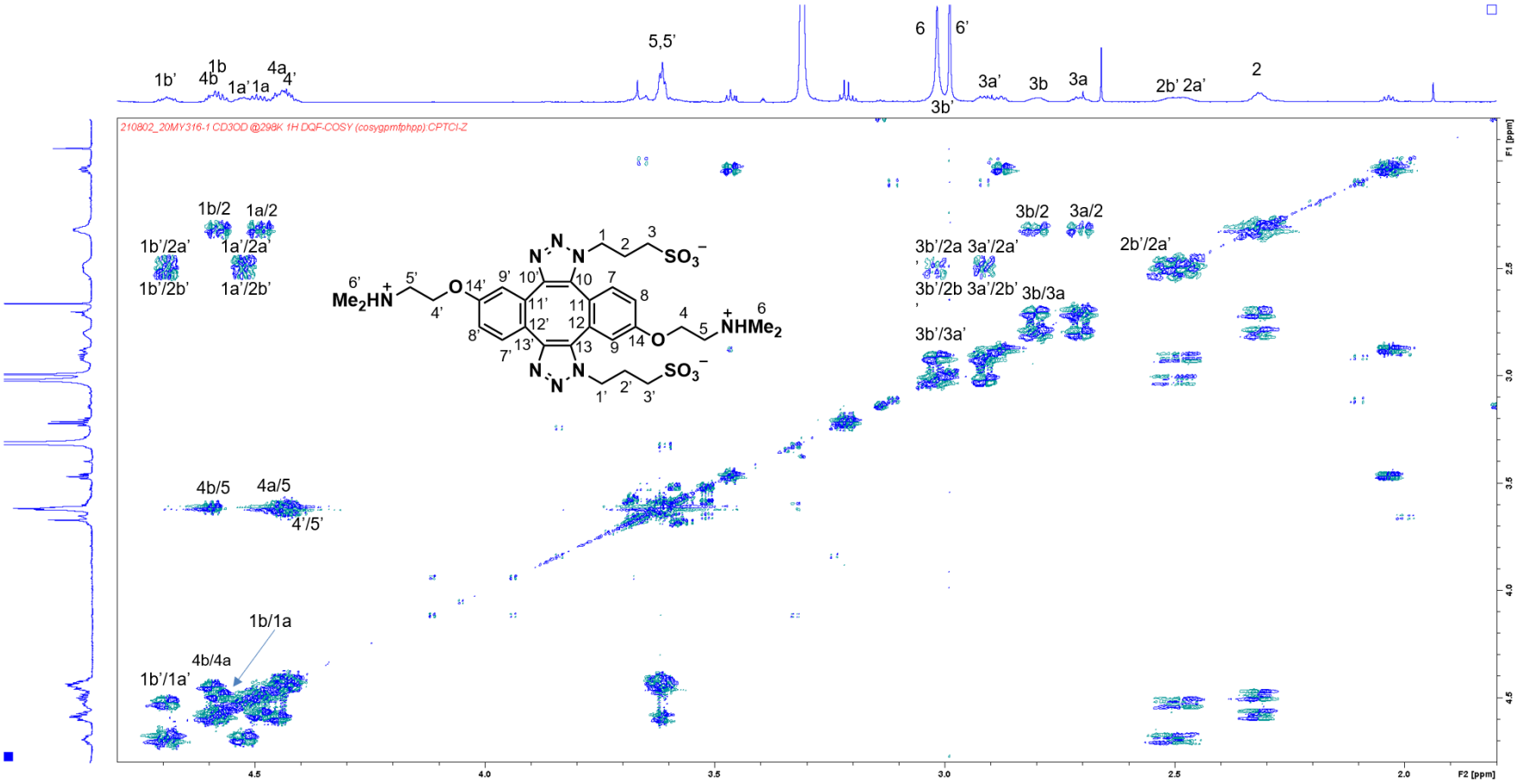

COSY spectrum of **5a**.

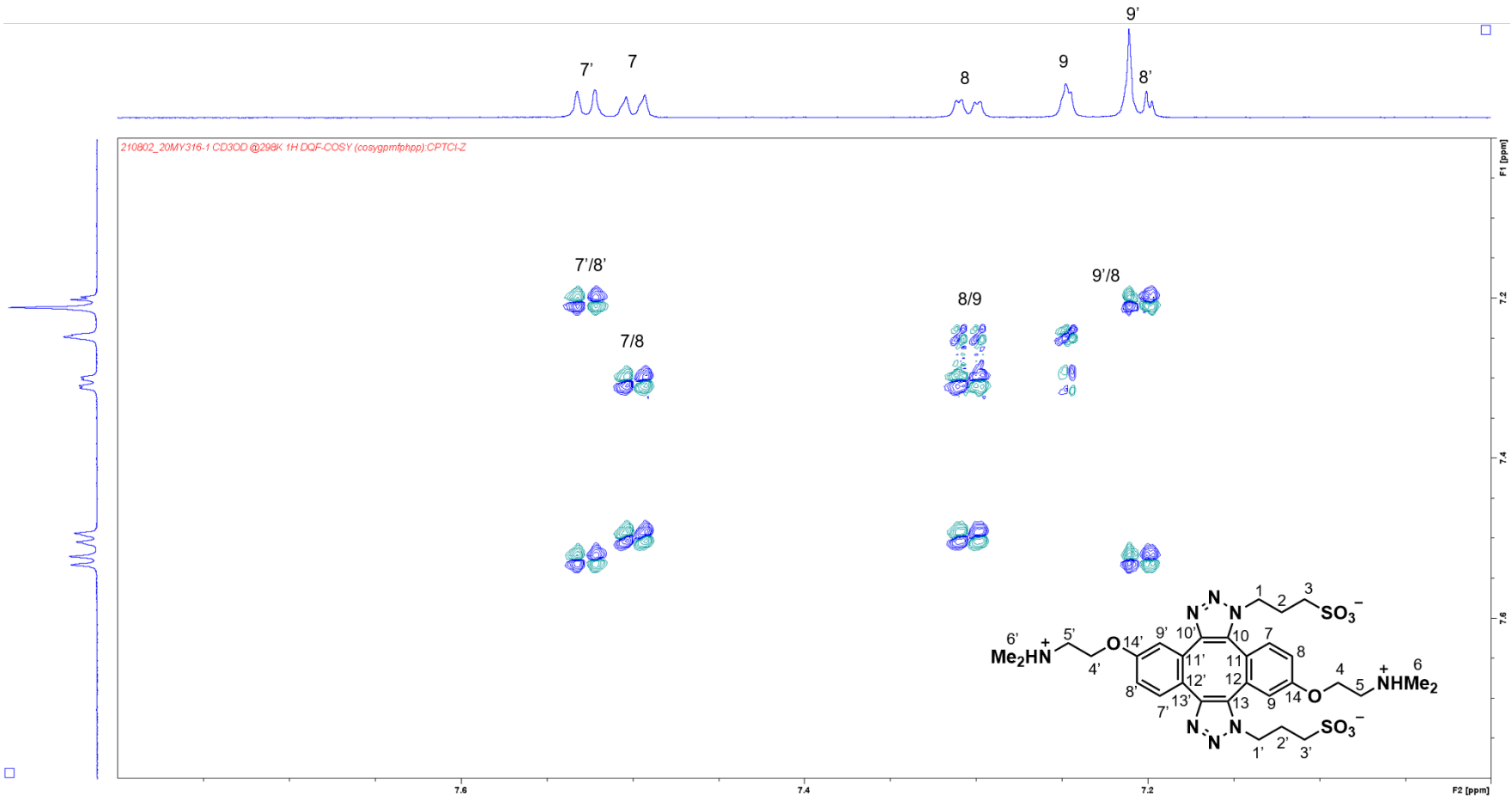

HSQC (blue/green) and HMBC (red) spectrum of **5a**.

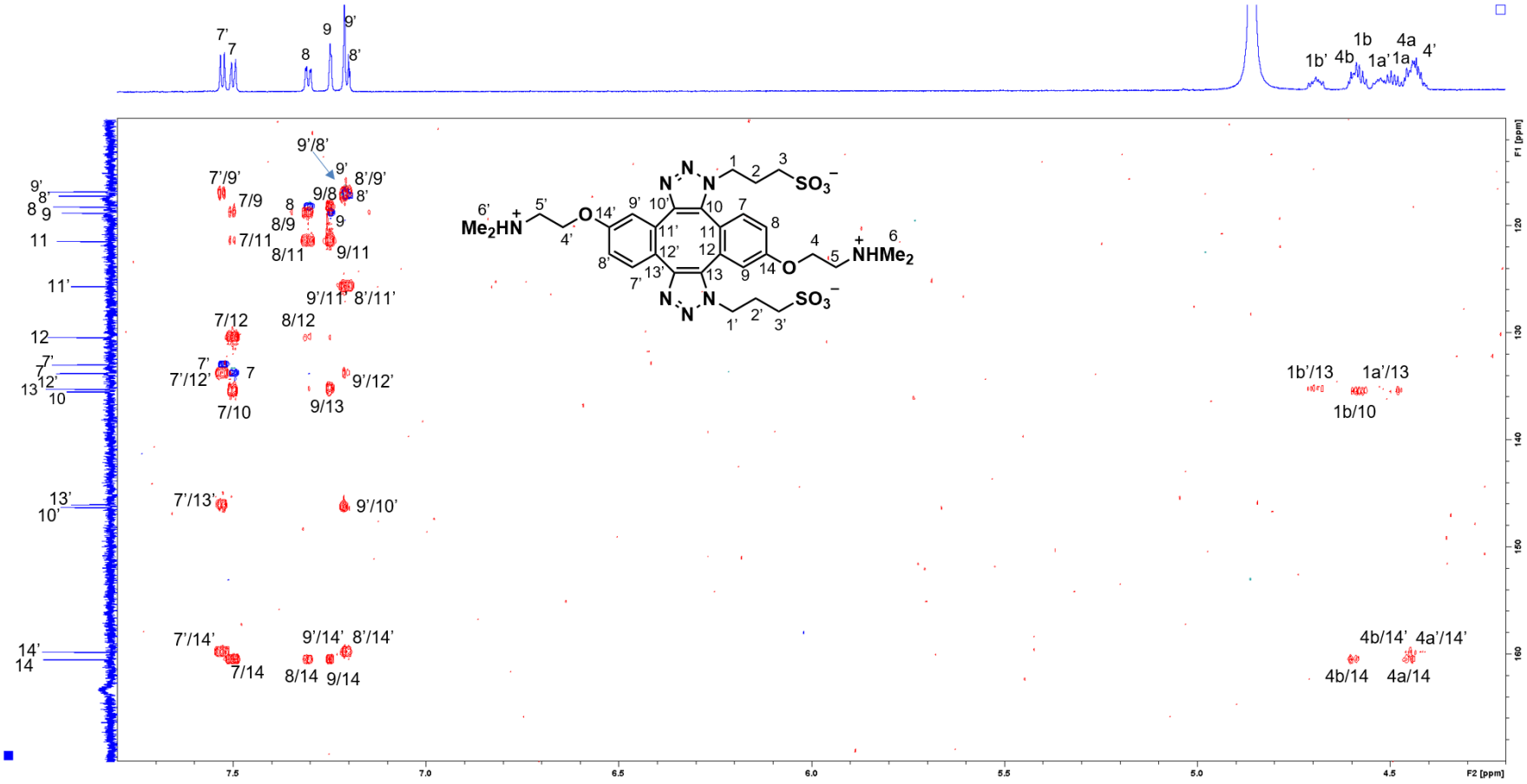

HSQC (blue/green) and HMBC (red) spectrum of **5a**.

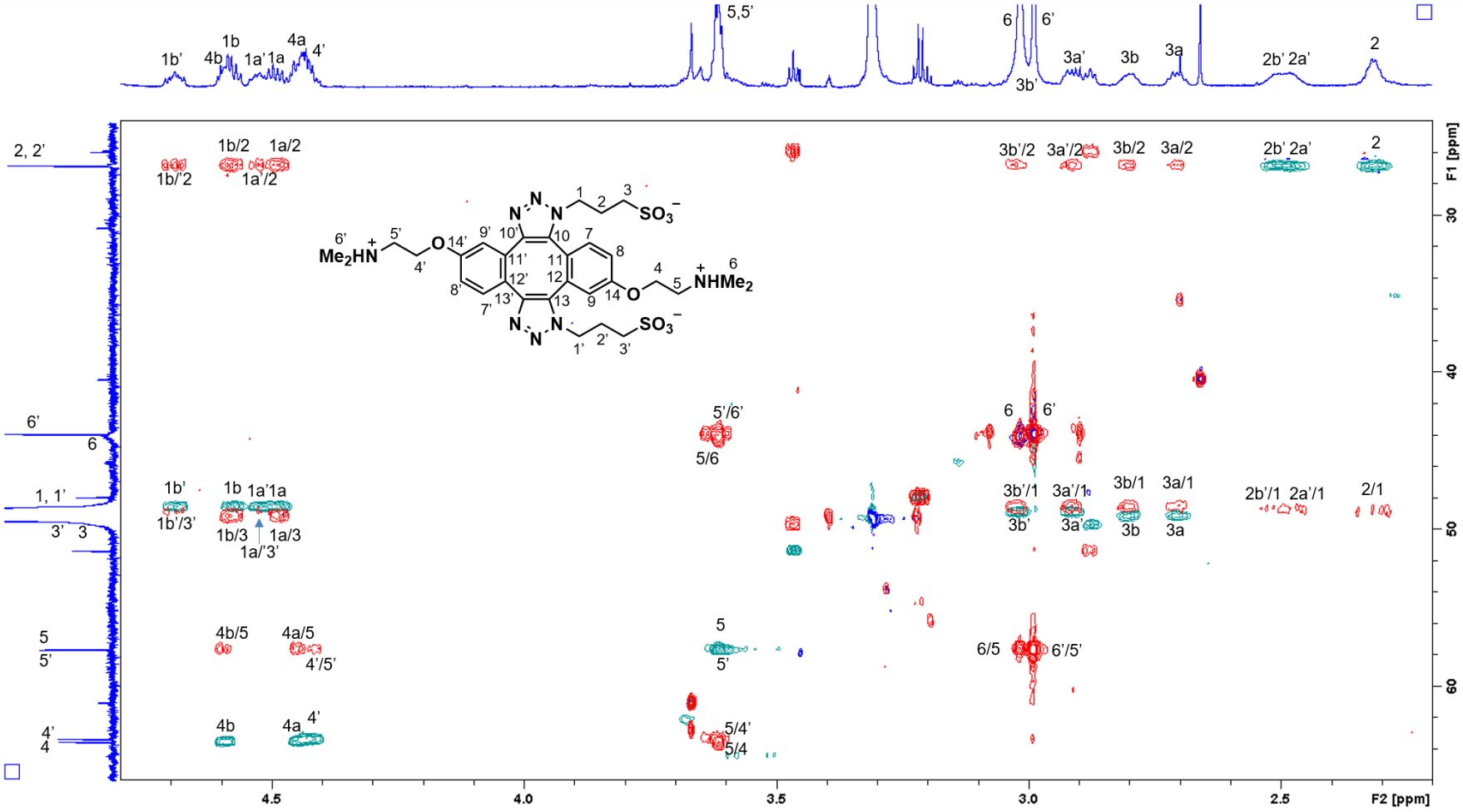

HSQC (blue/green) and HMBC (red) spectrum of **5a**.

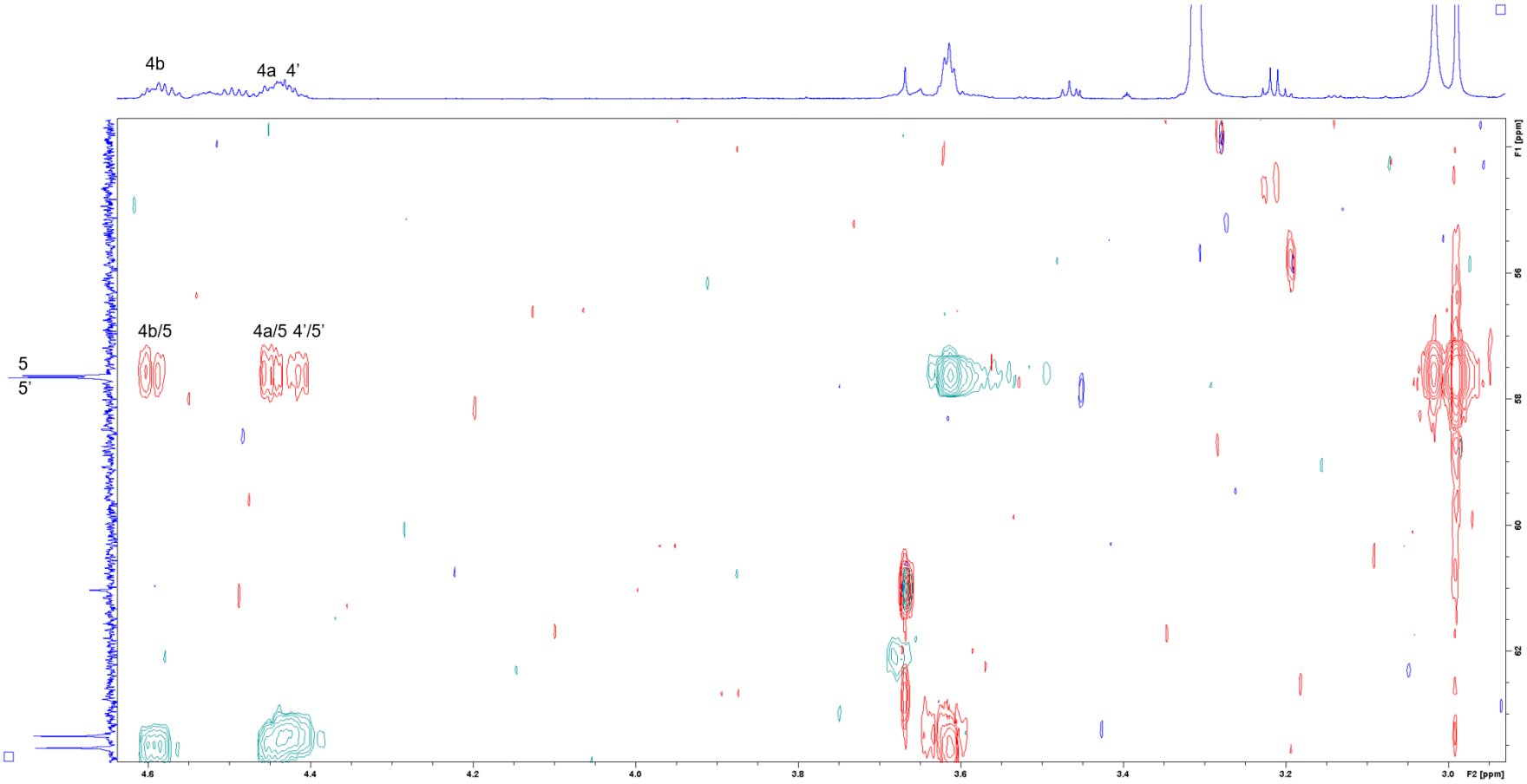

NOESY spectrum of **5a**. (mixing time: 1000 ms)

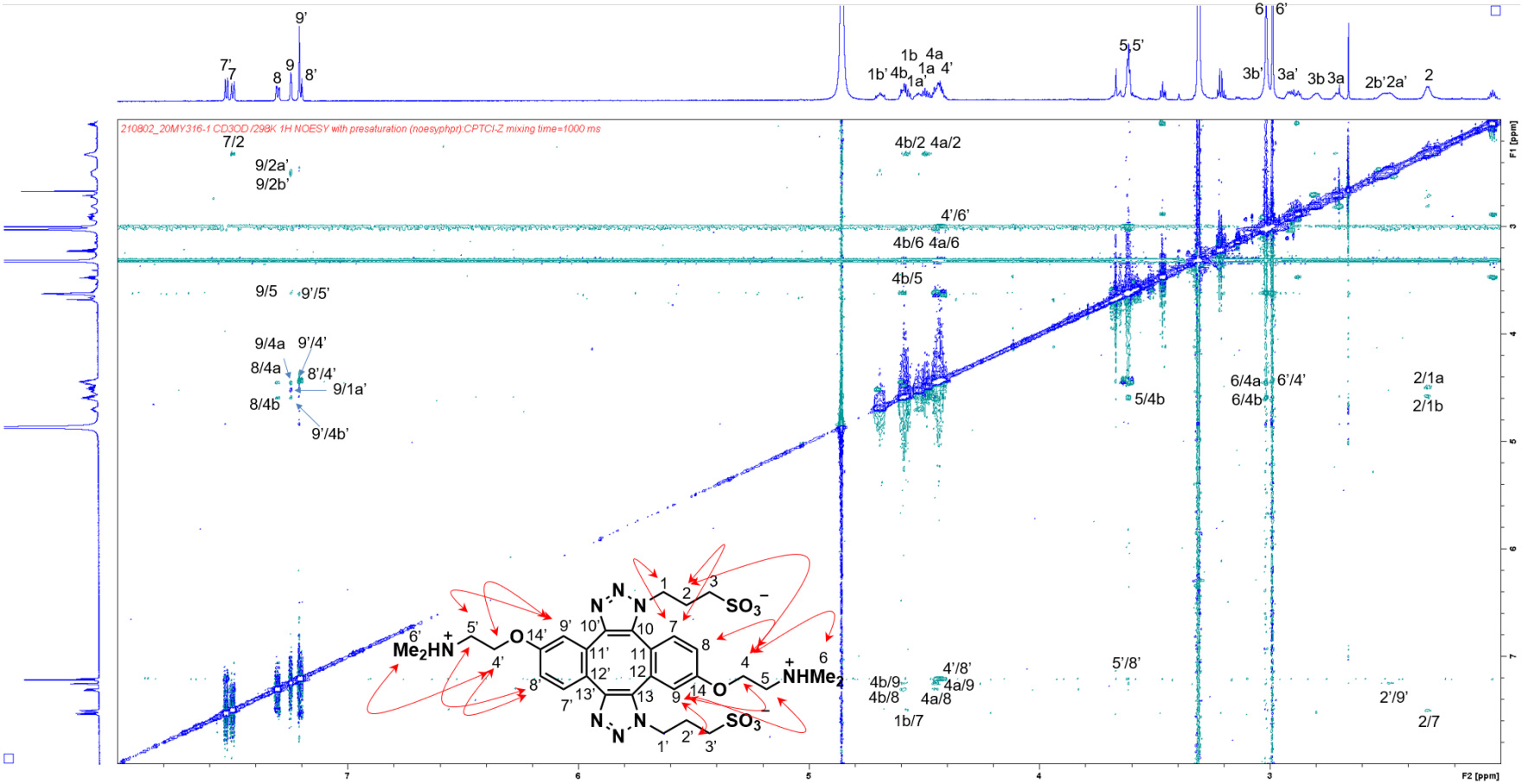

ROESY spectrum of **5a**. (mixing time: 200 ms)

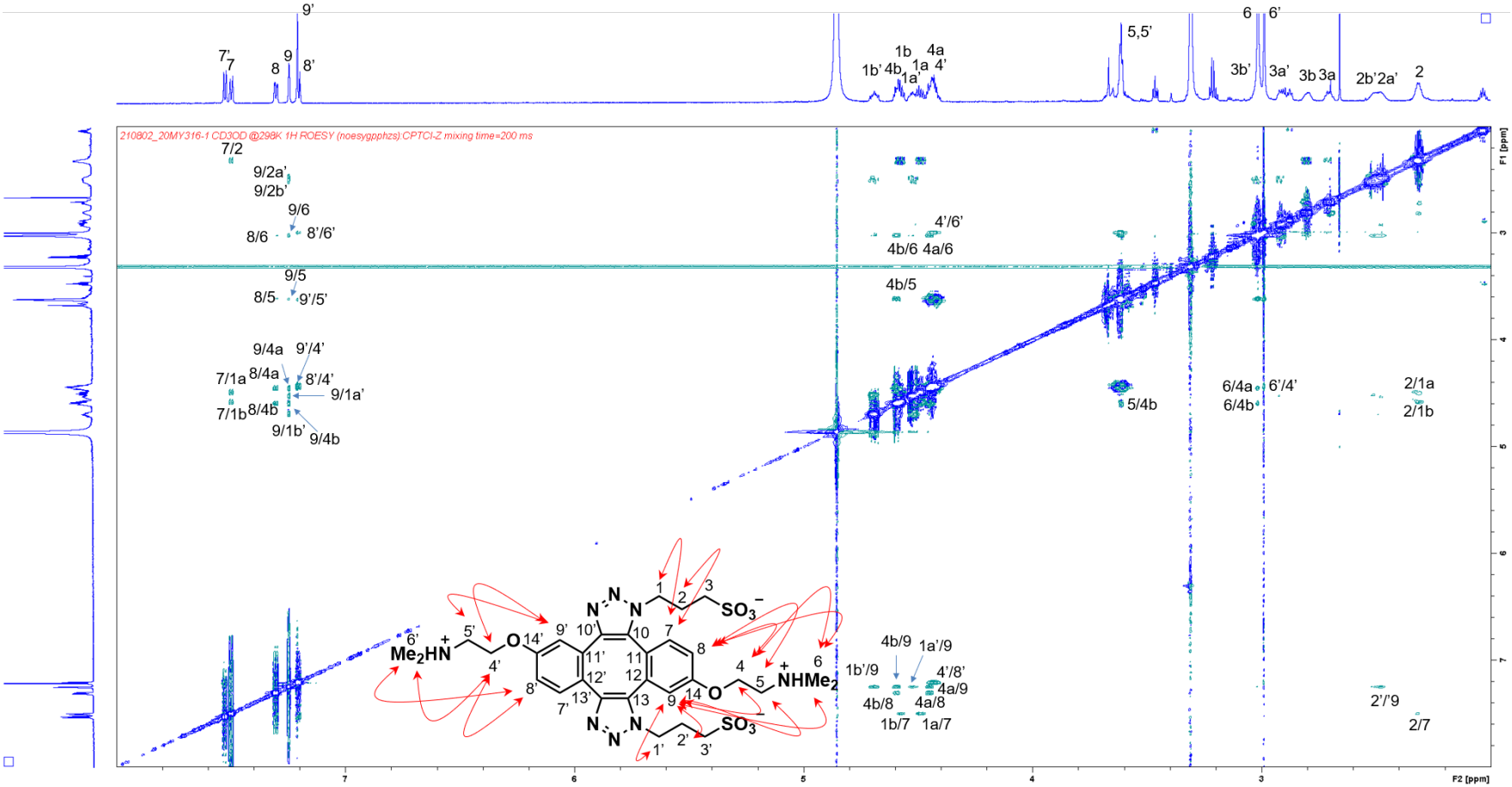

^{1}H NMR spectrum of **5b**.

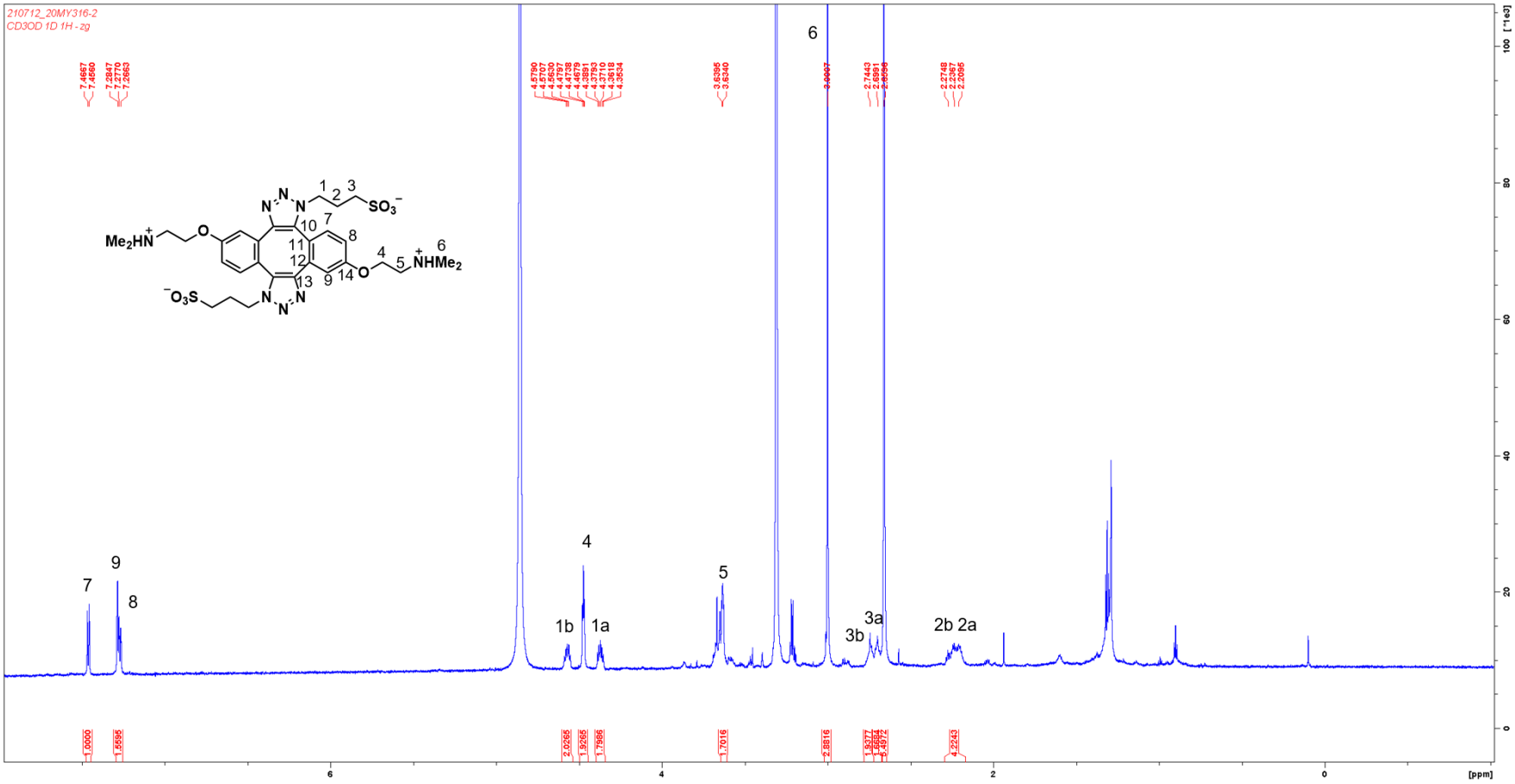

^{13}C NMR spectrum of **5b**.

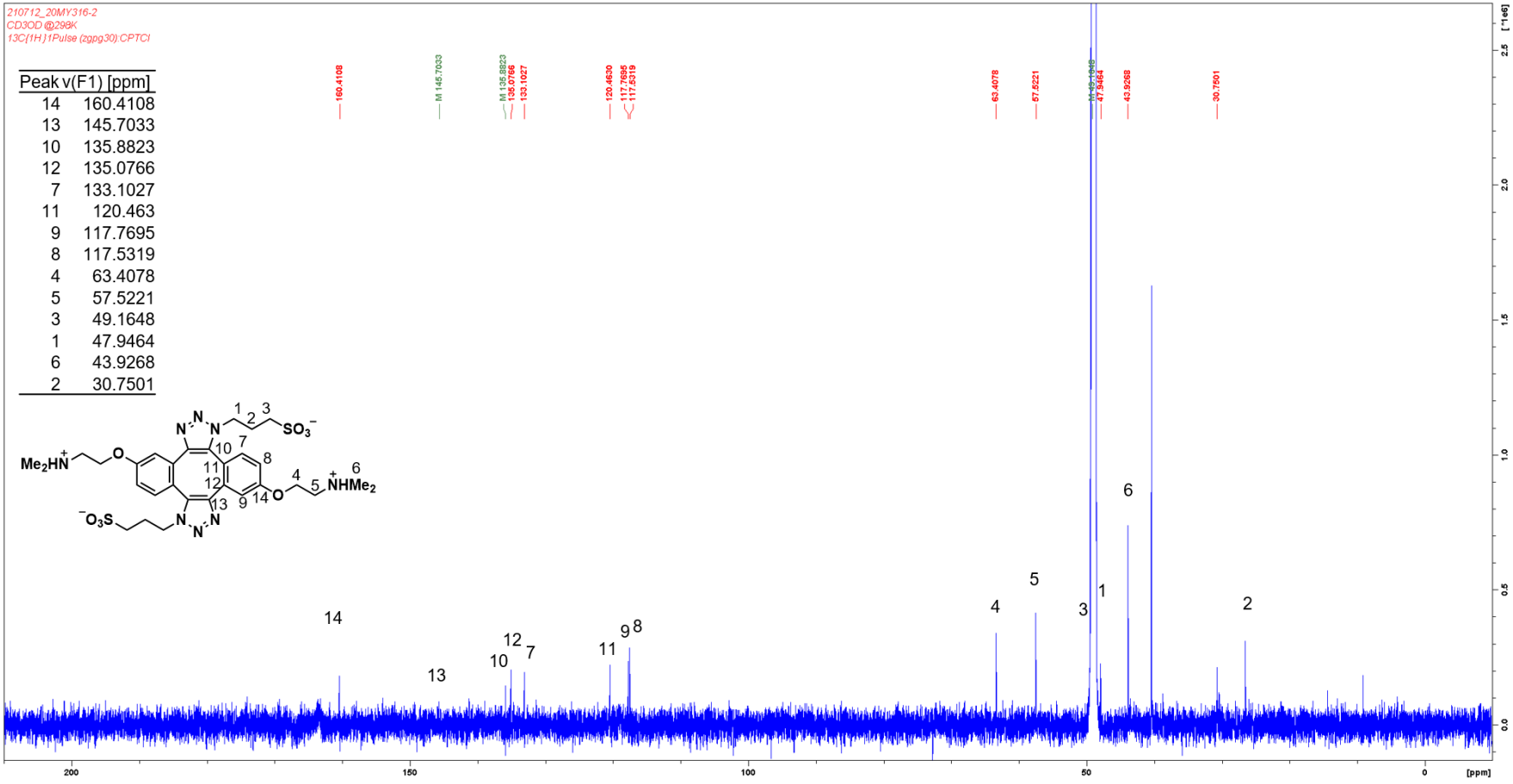

COSY spectrum of **5b**.

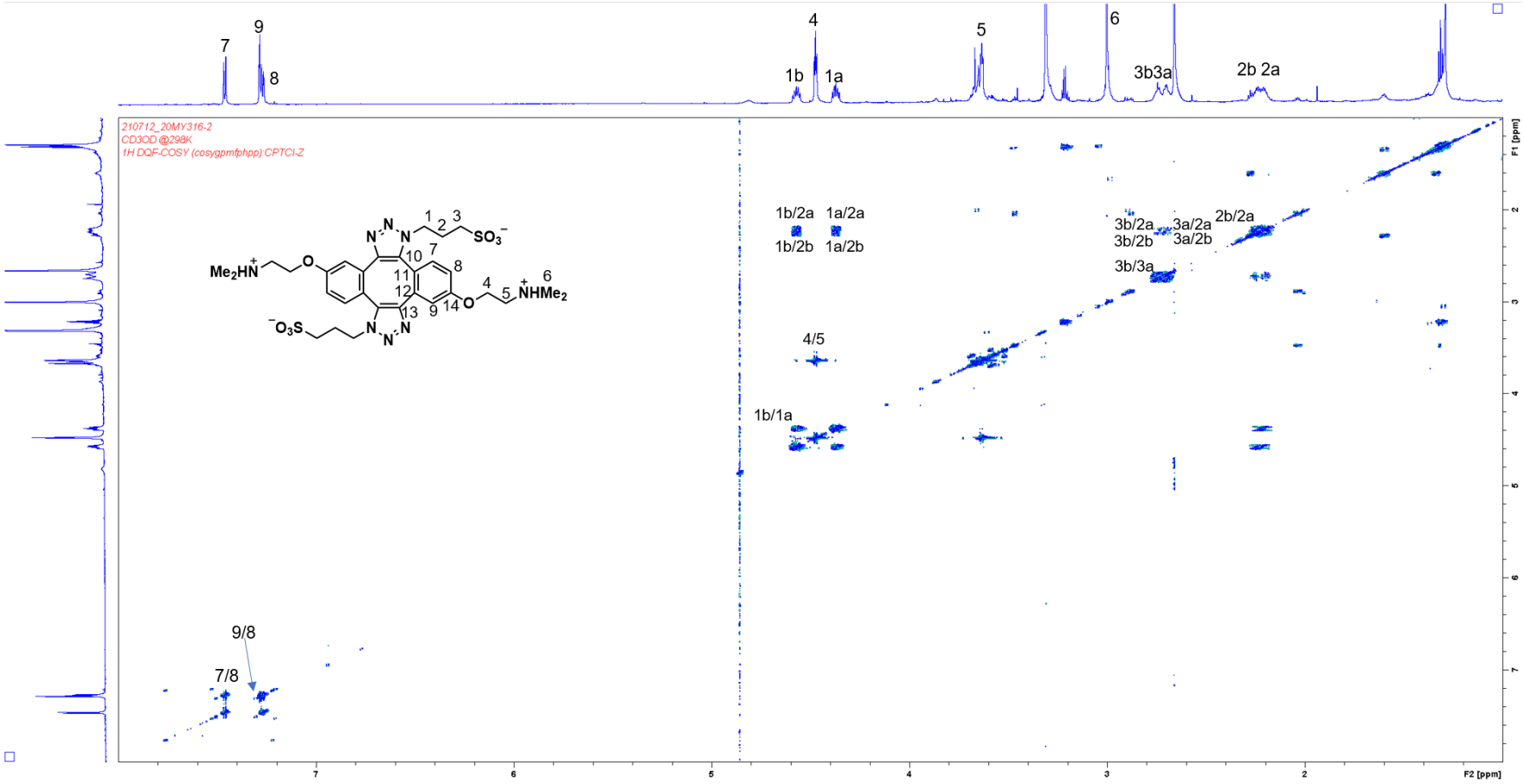

HSQC (blue/green) and HMBC (red) spectrum of **5b**.

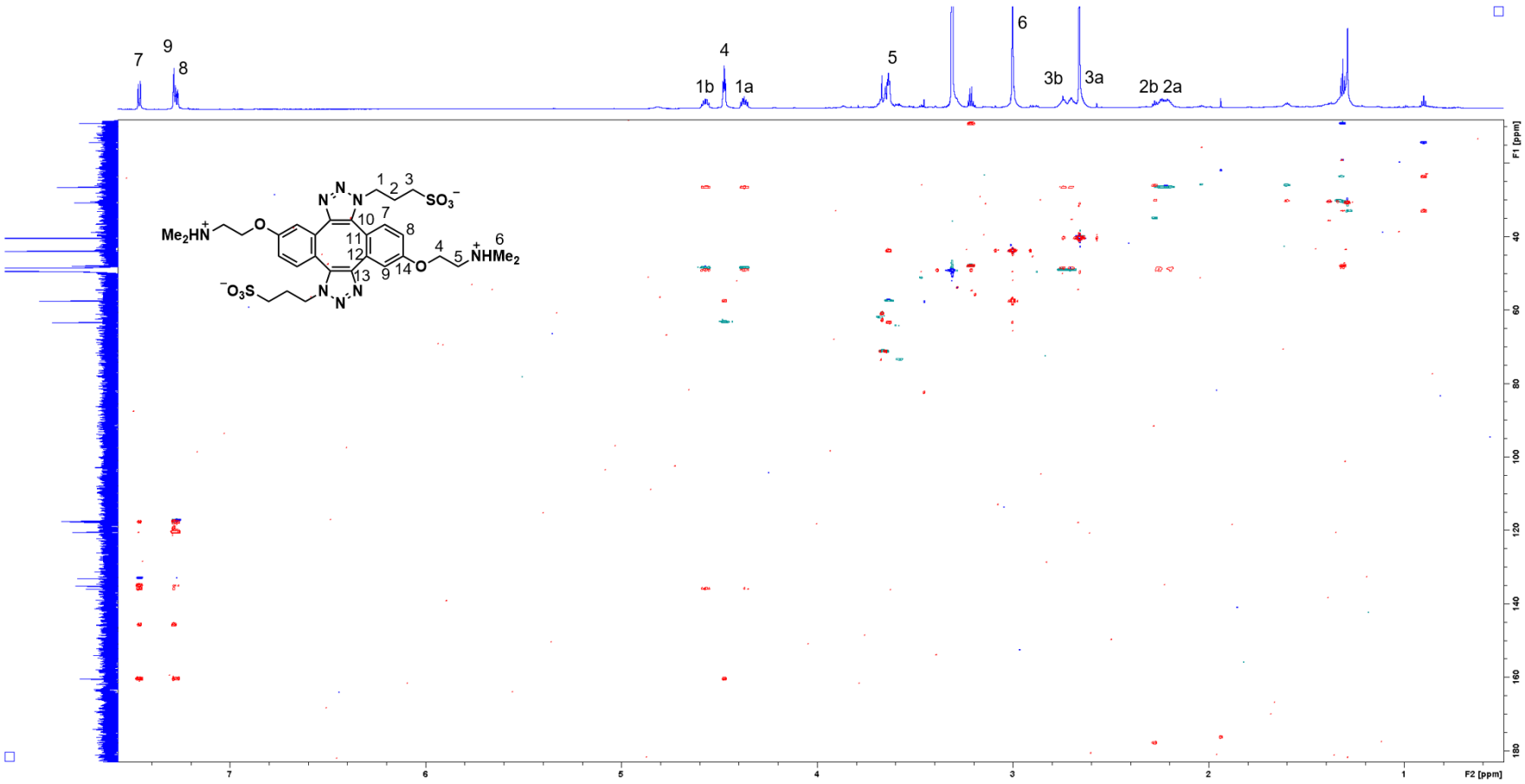

HSQC (blue/green) and HMBC (red) spectrum of **5b**.

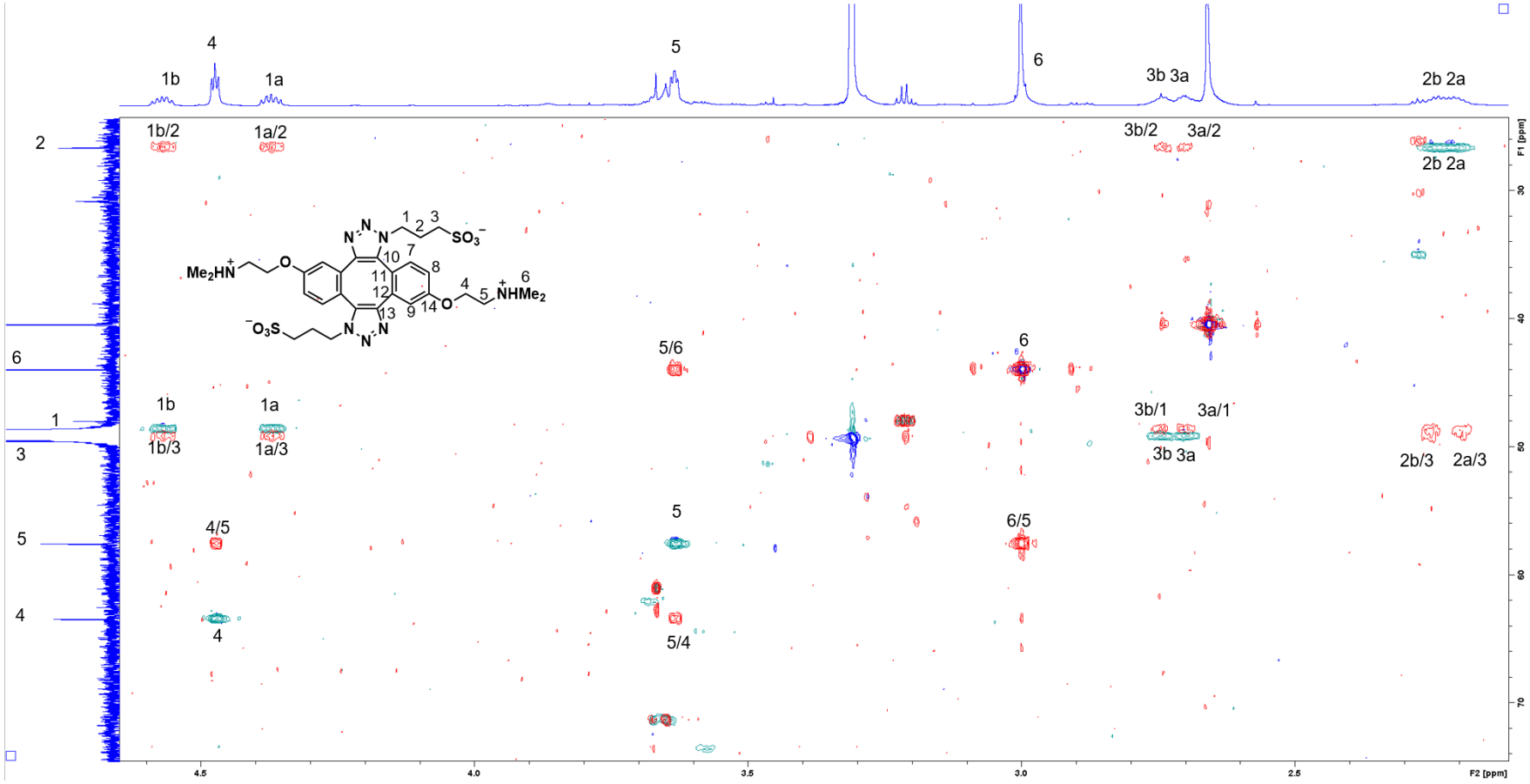

HSQC (blue/green) and HMBC (red) spectrum of **5b**.

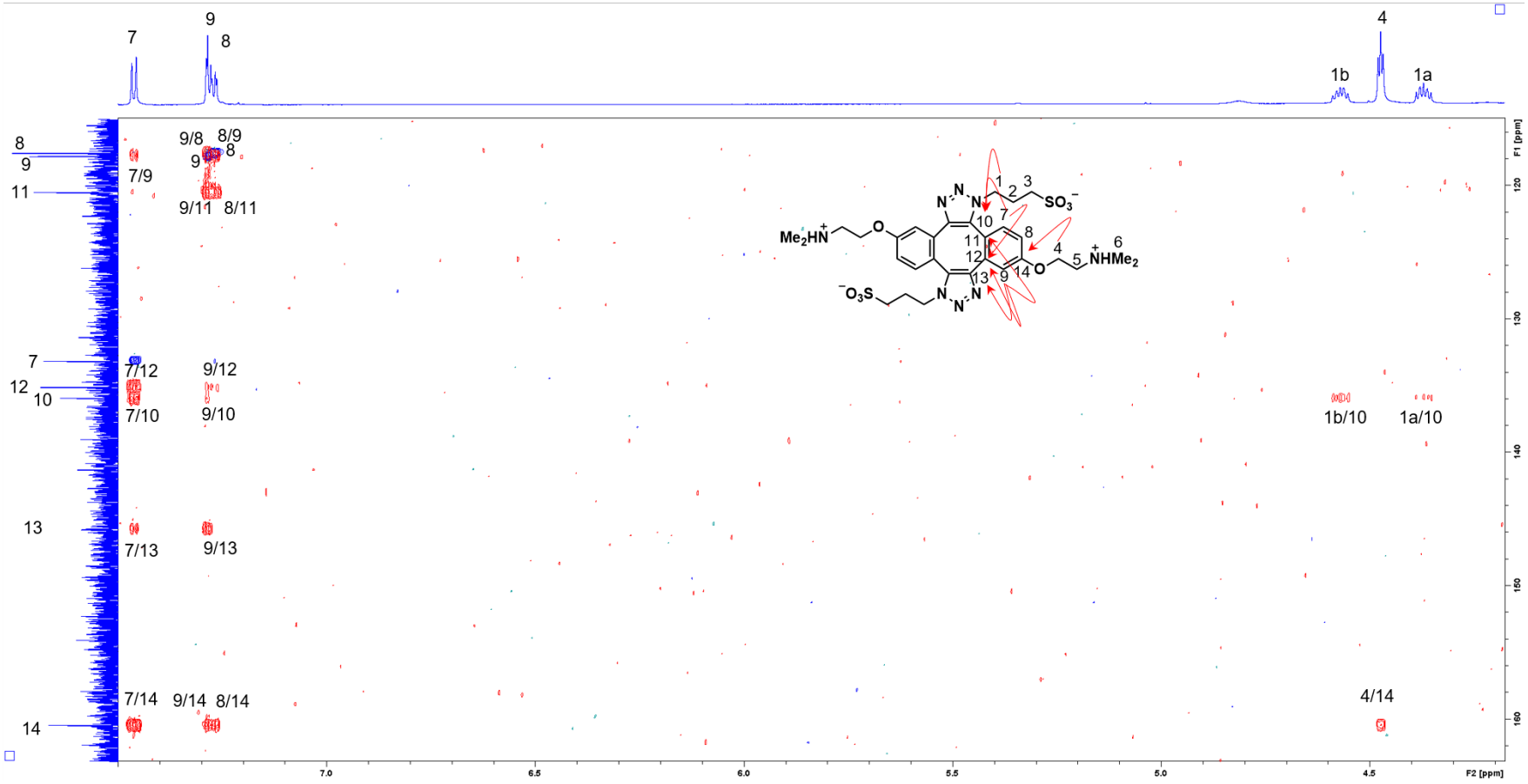

NOESY spectrum of **5b**. (mixing time: 500 ms)

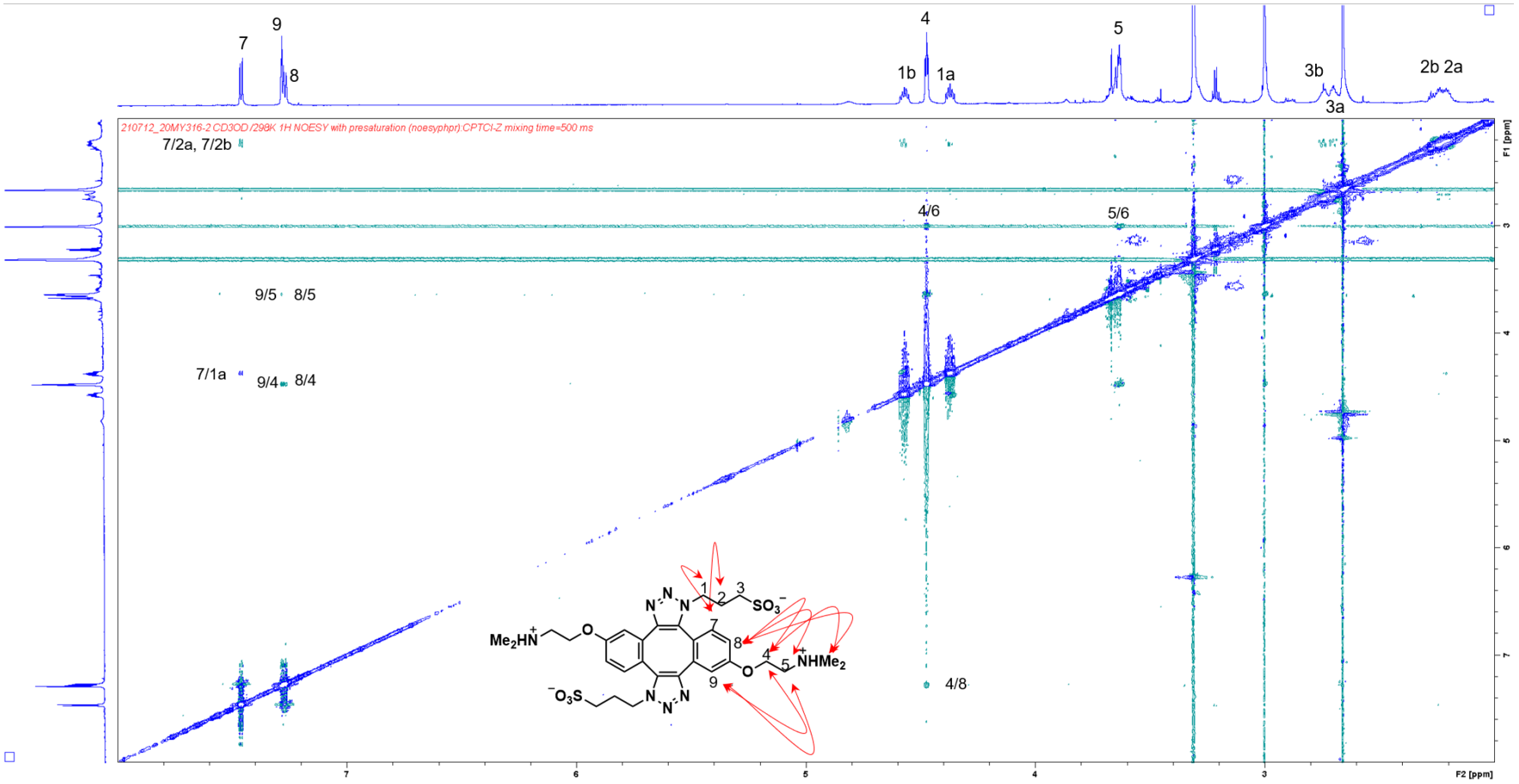

ROESY spectrum of **5b**. (mixing time: 200 ms)

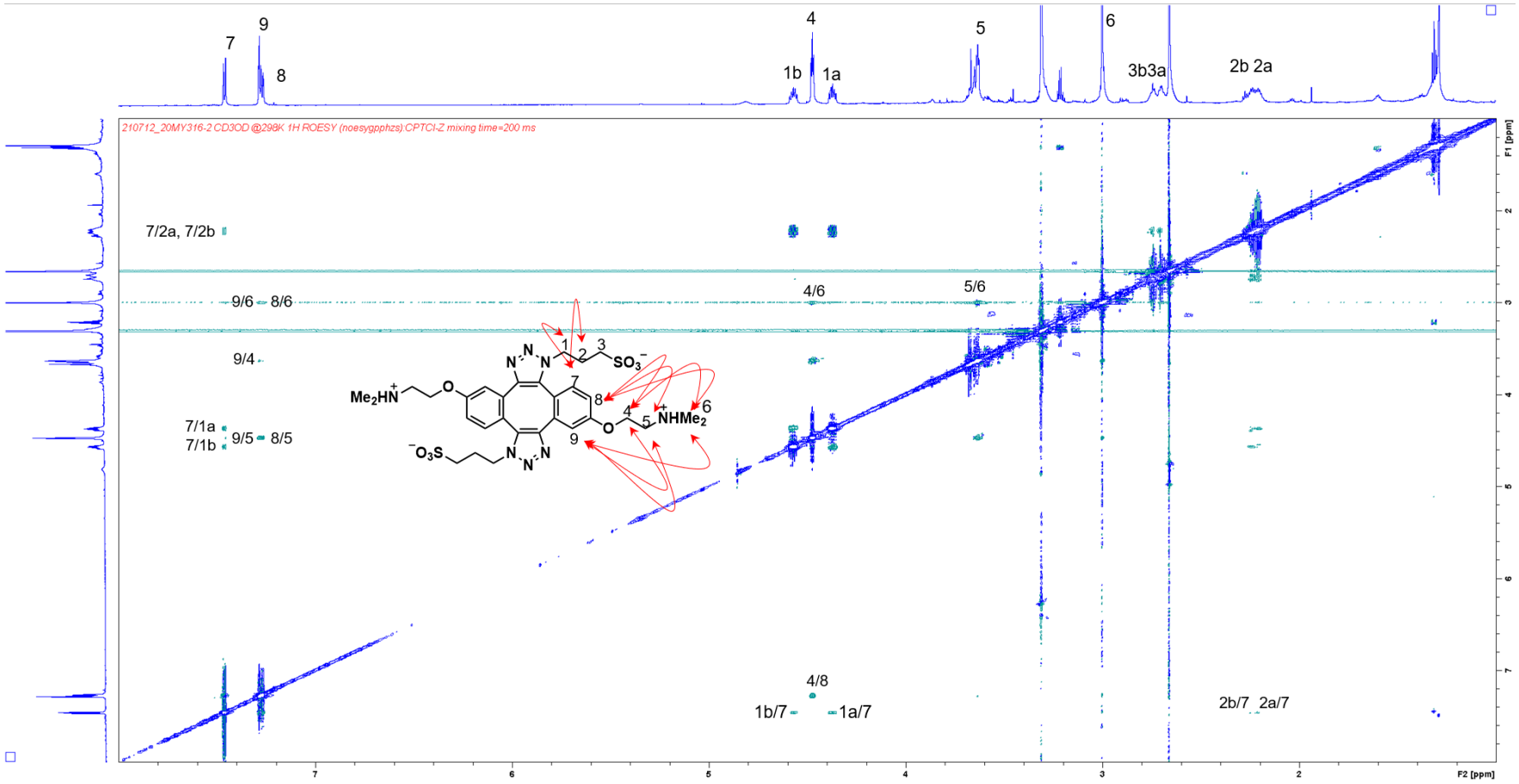

^{1}H NMR spectrum of **5c**.

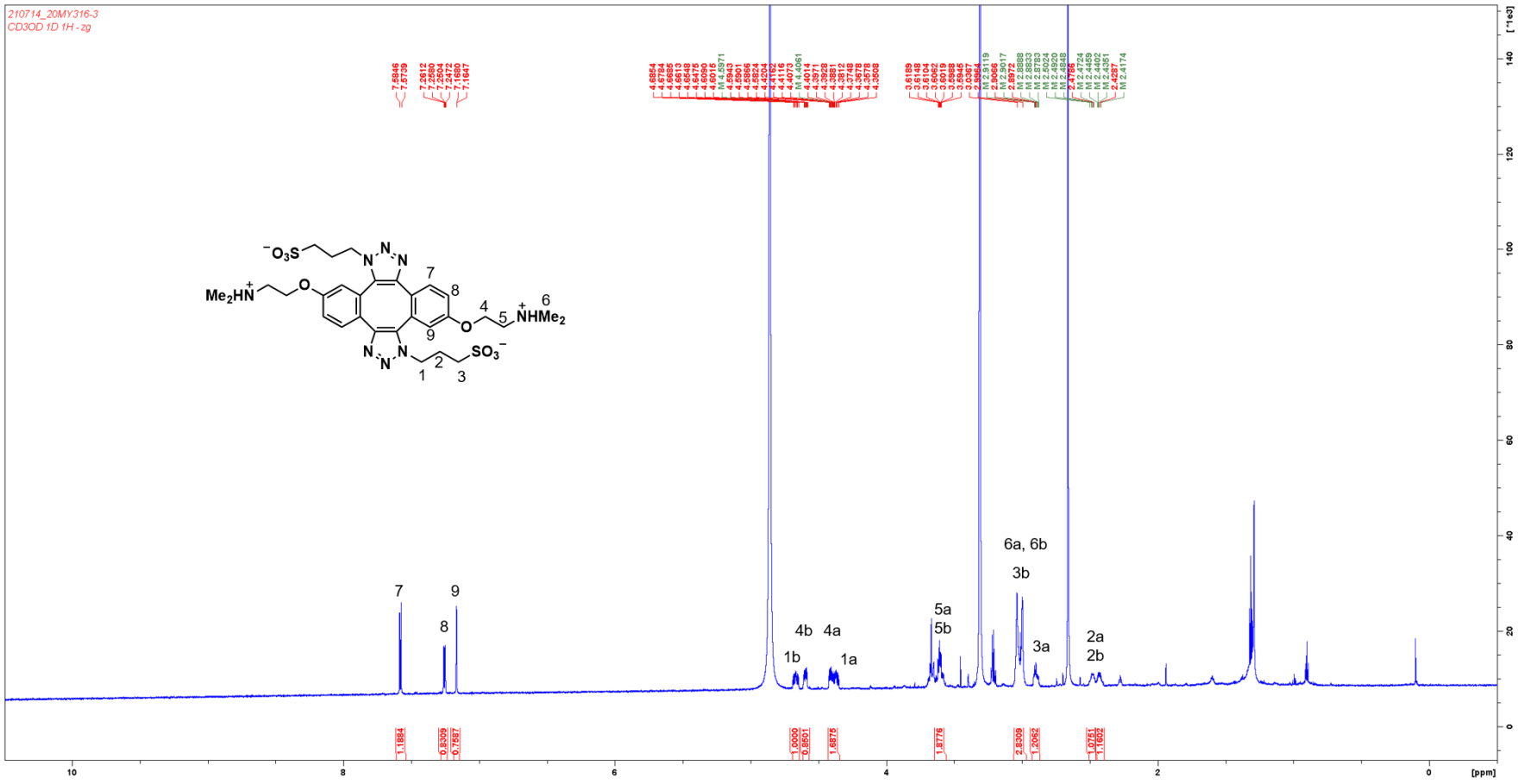

^{13}C NMR spectrum of **5c**.

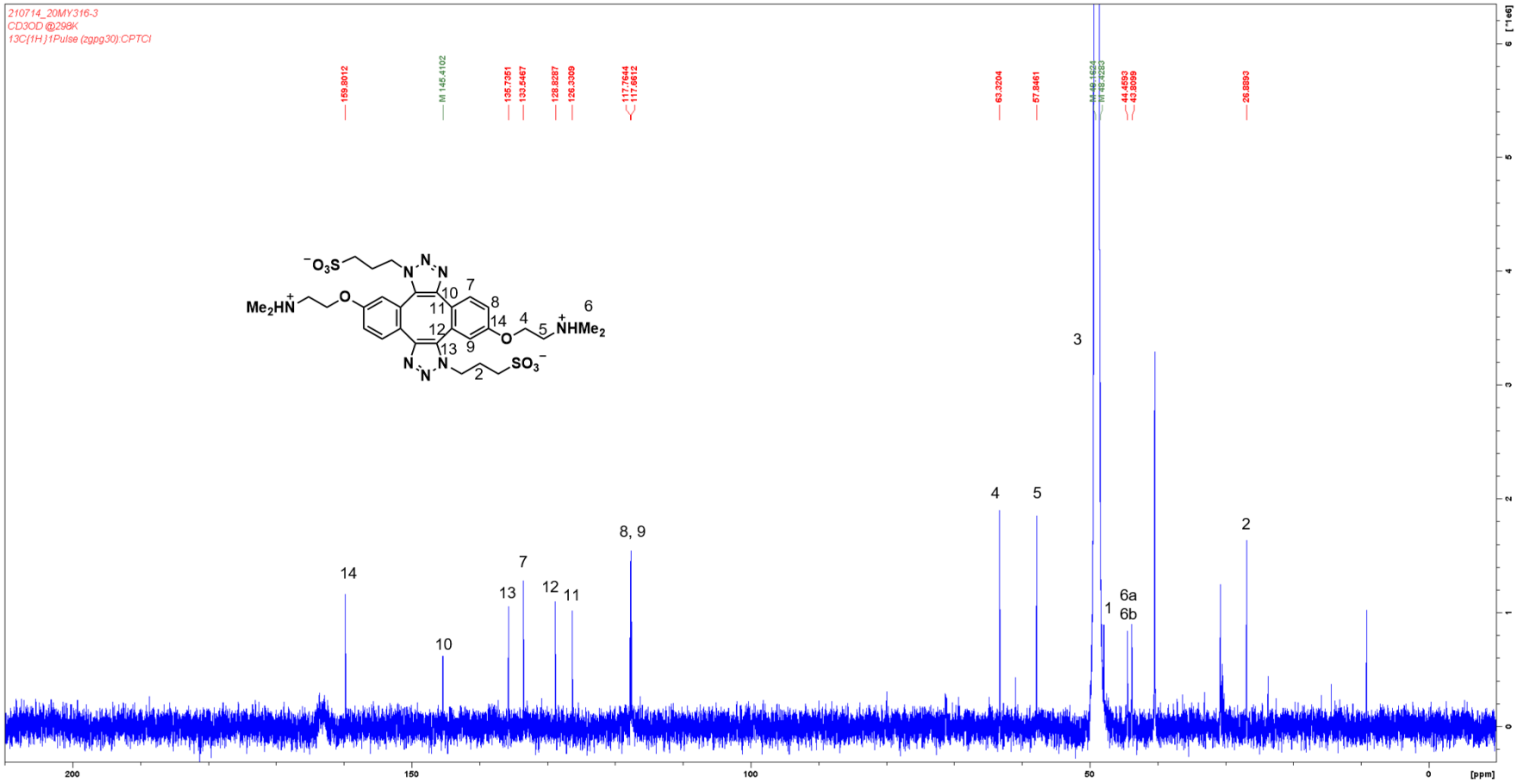

COSY spectrum of **5c**.

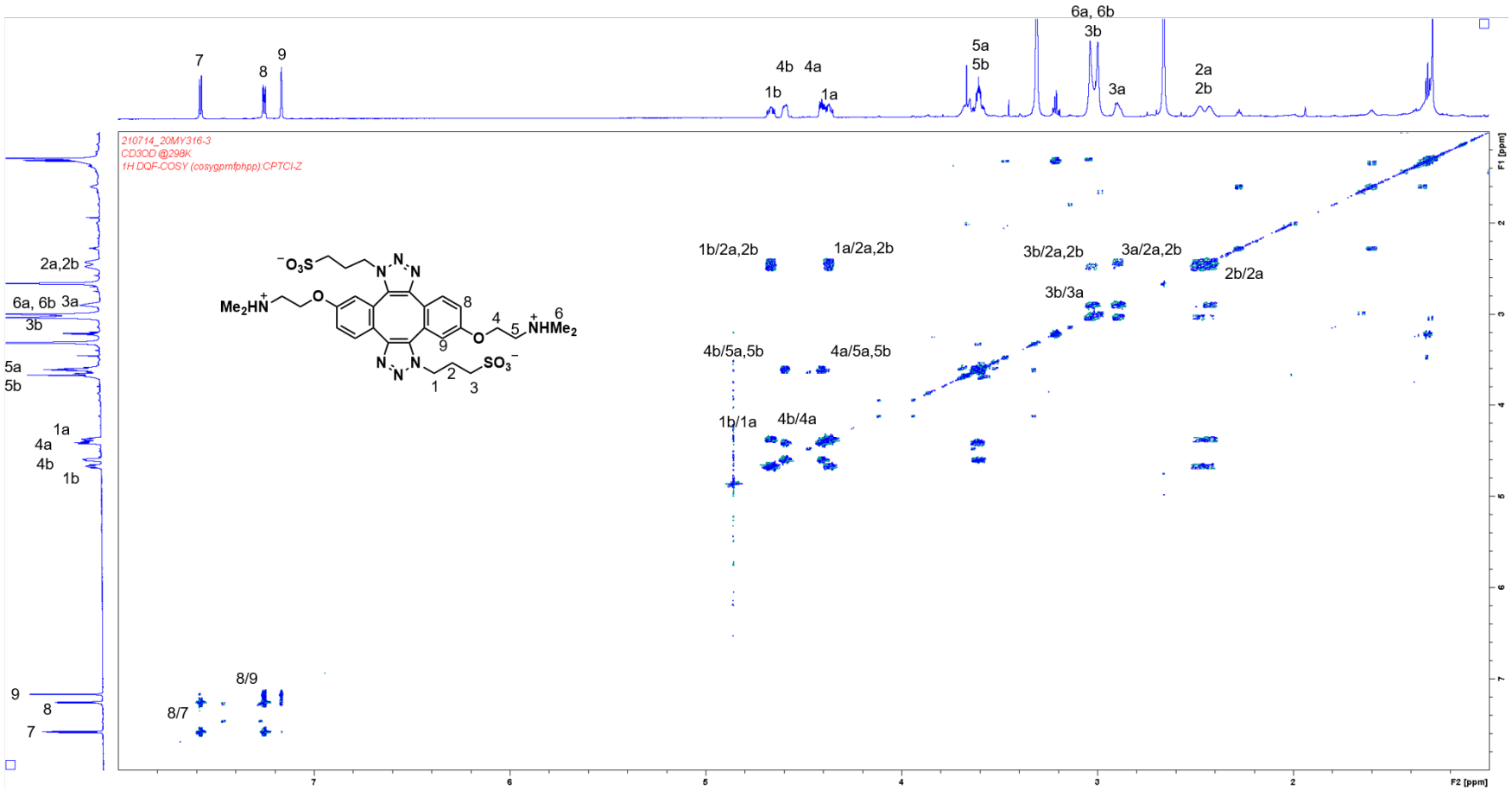

HSQC (blue/green) and HMBC (red) spectrum of **5c**.

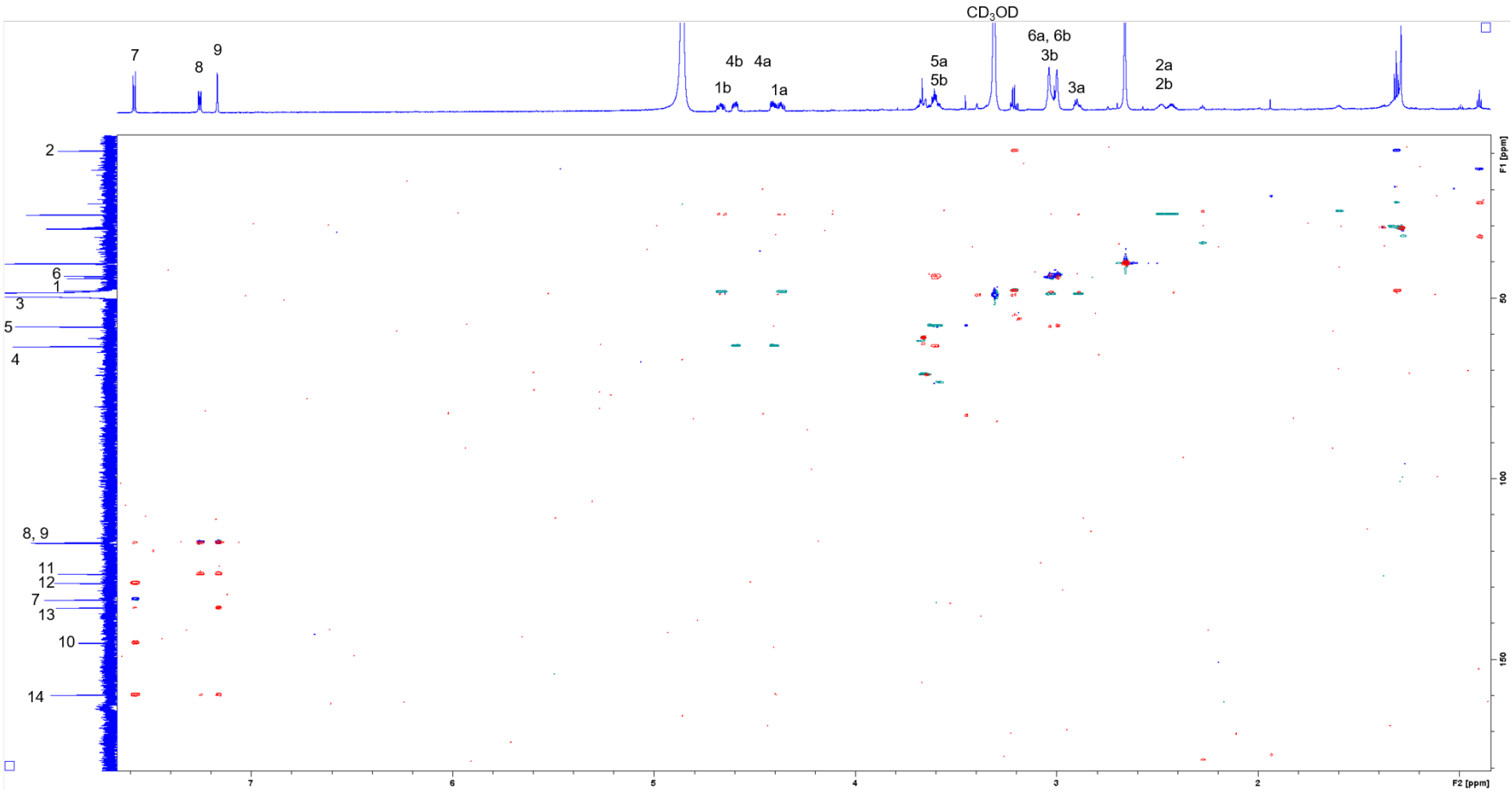

HSQC (blue/green) and HMBC (red) spectrum of **5c**.

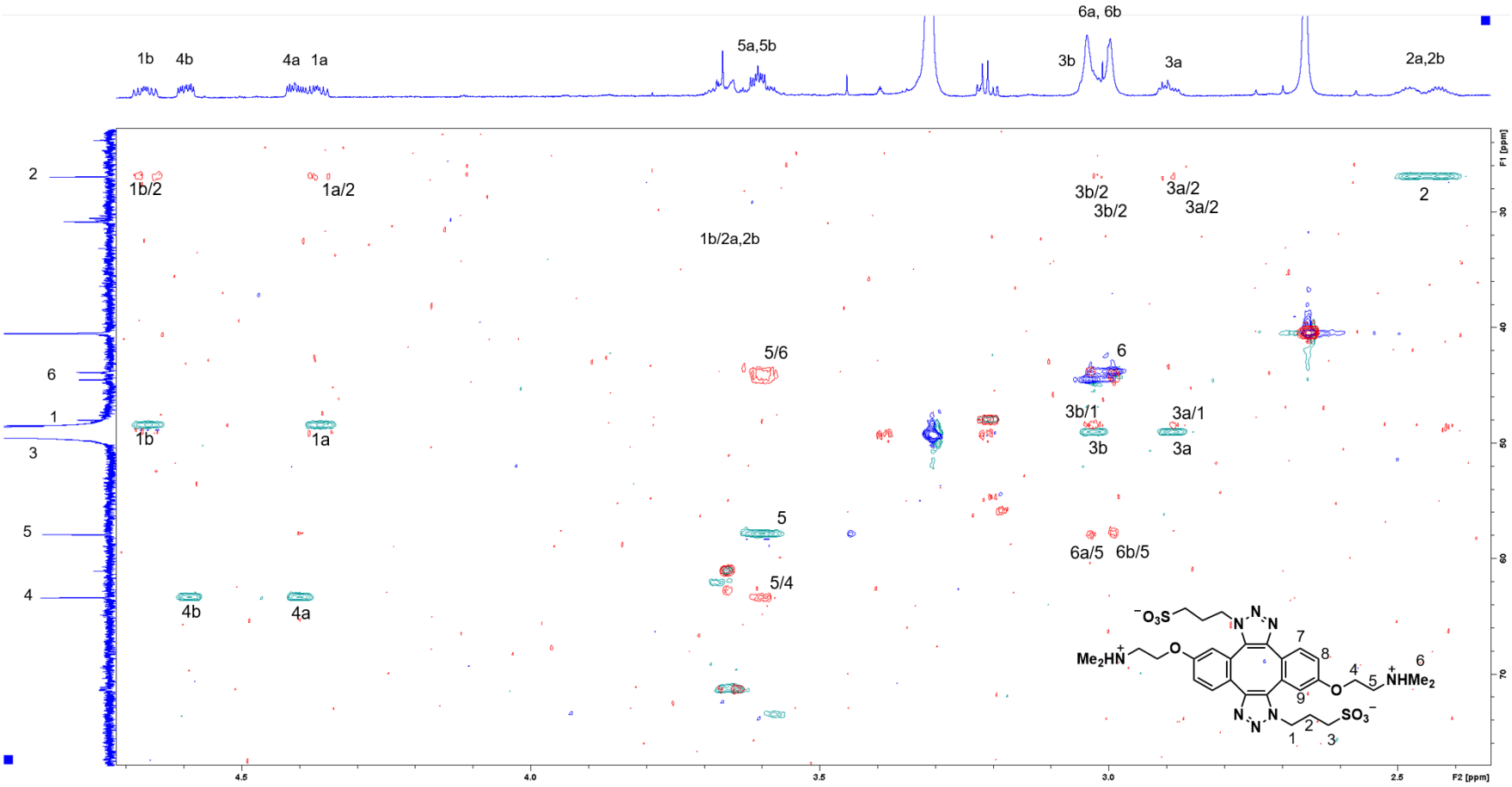

HSQC (blue/green) and HMBC (red) spectrum of **5c**.

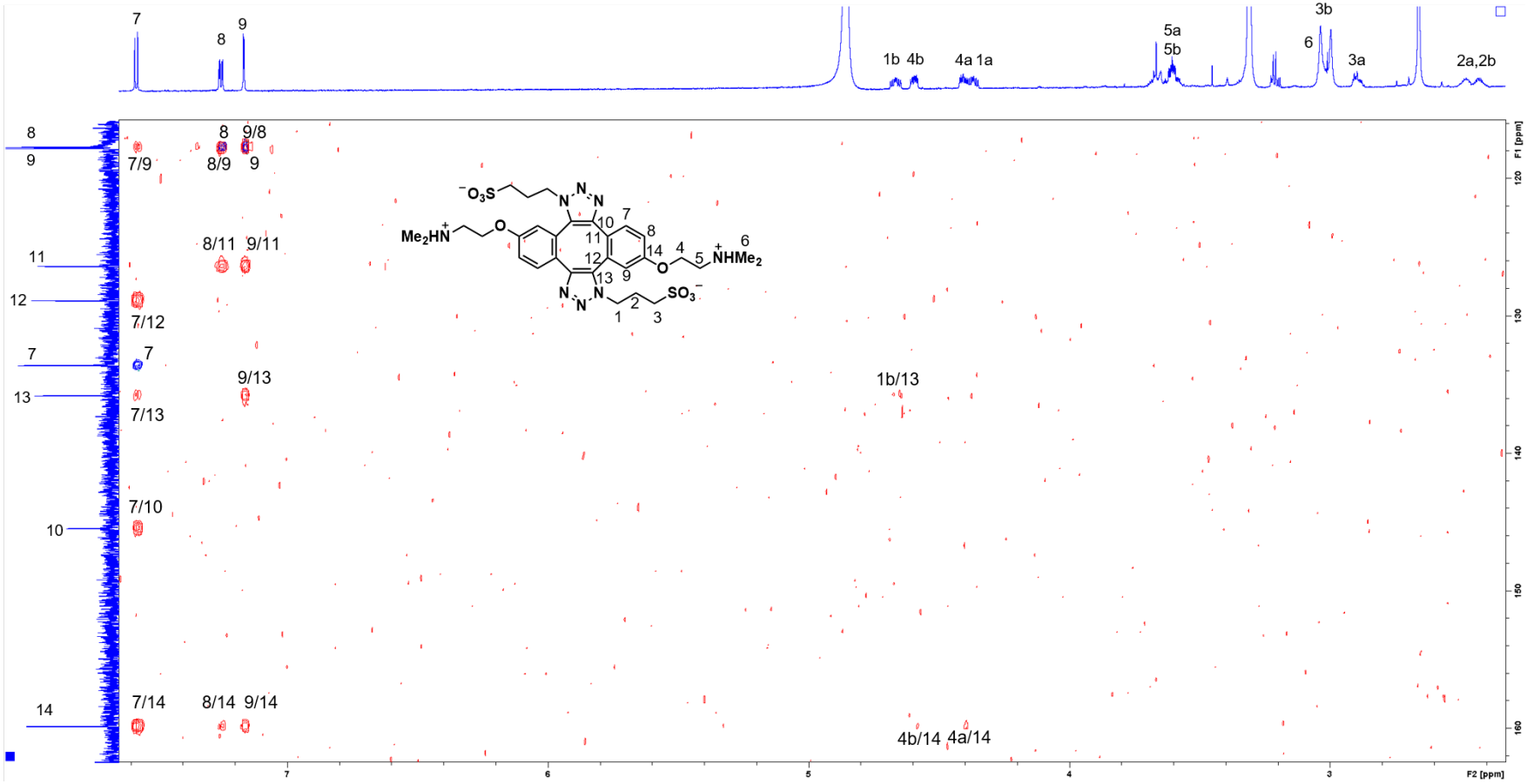

NOESY spectrum of **5c**. (mixing time: 500 ms)

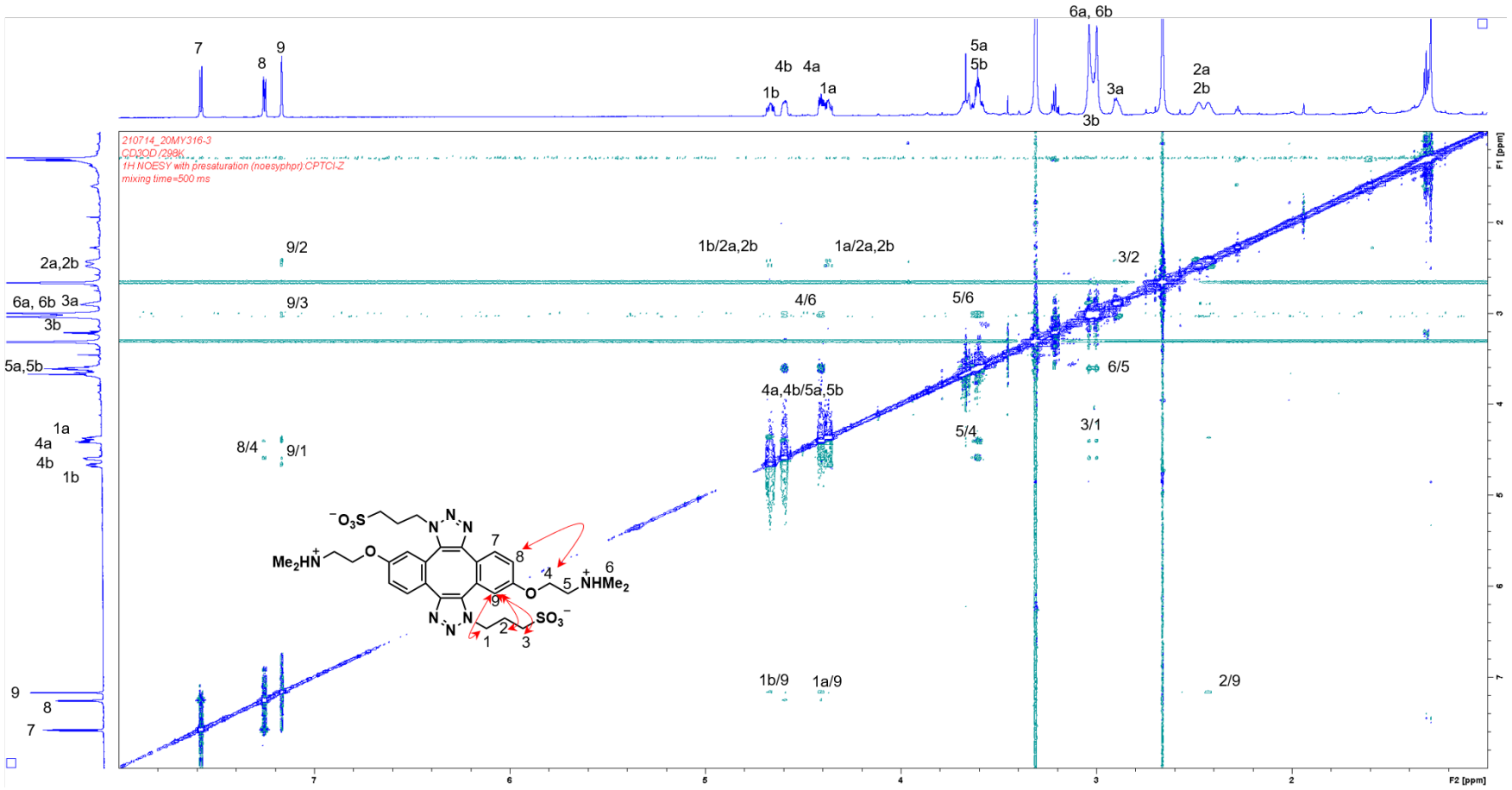

ROESY spectrum of **5c**. (mixing time: 200 ms)

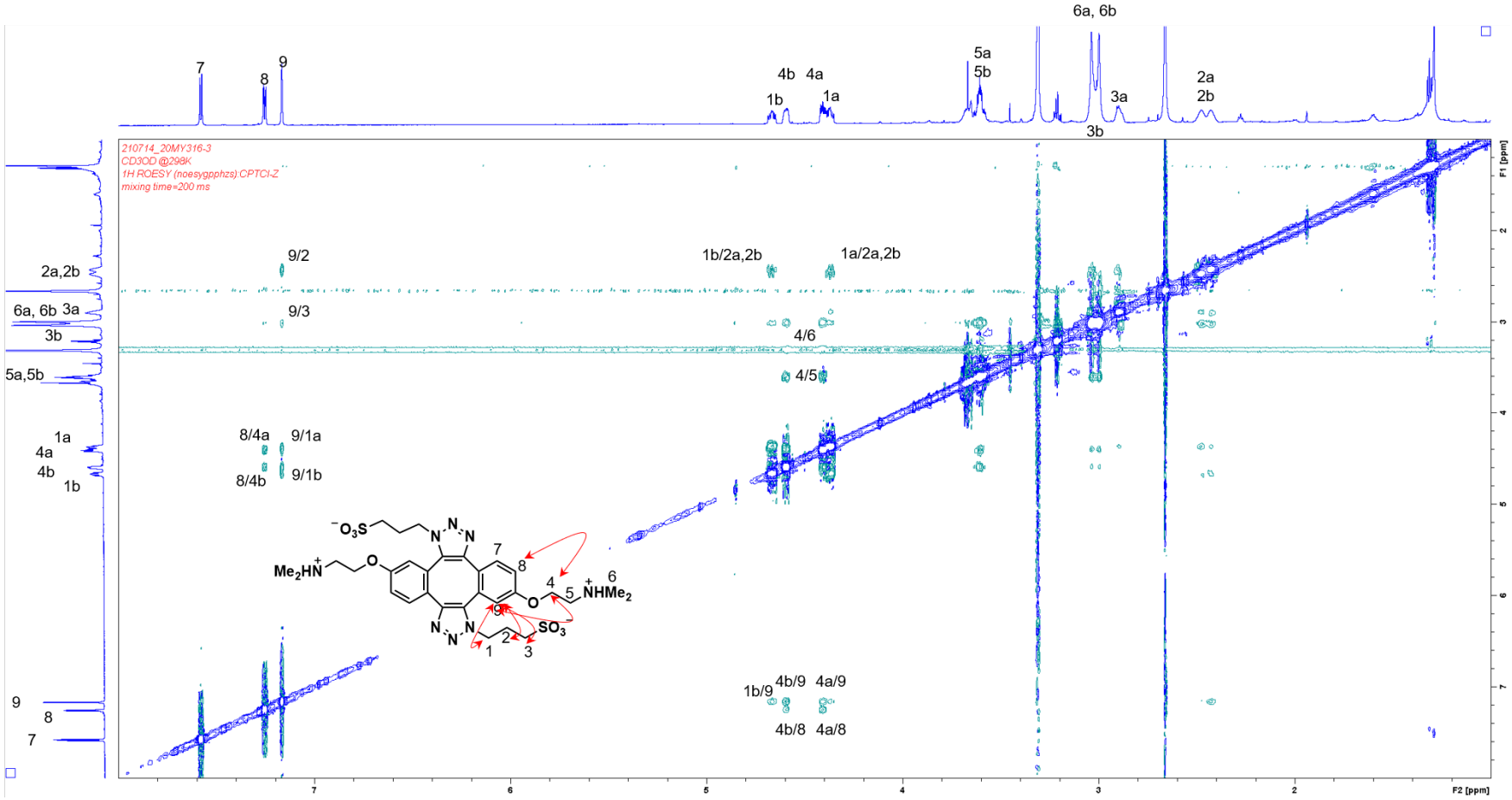

9. Whole gel images

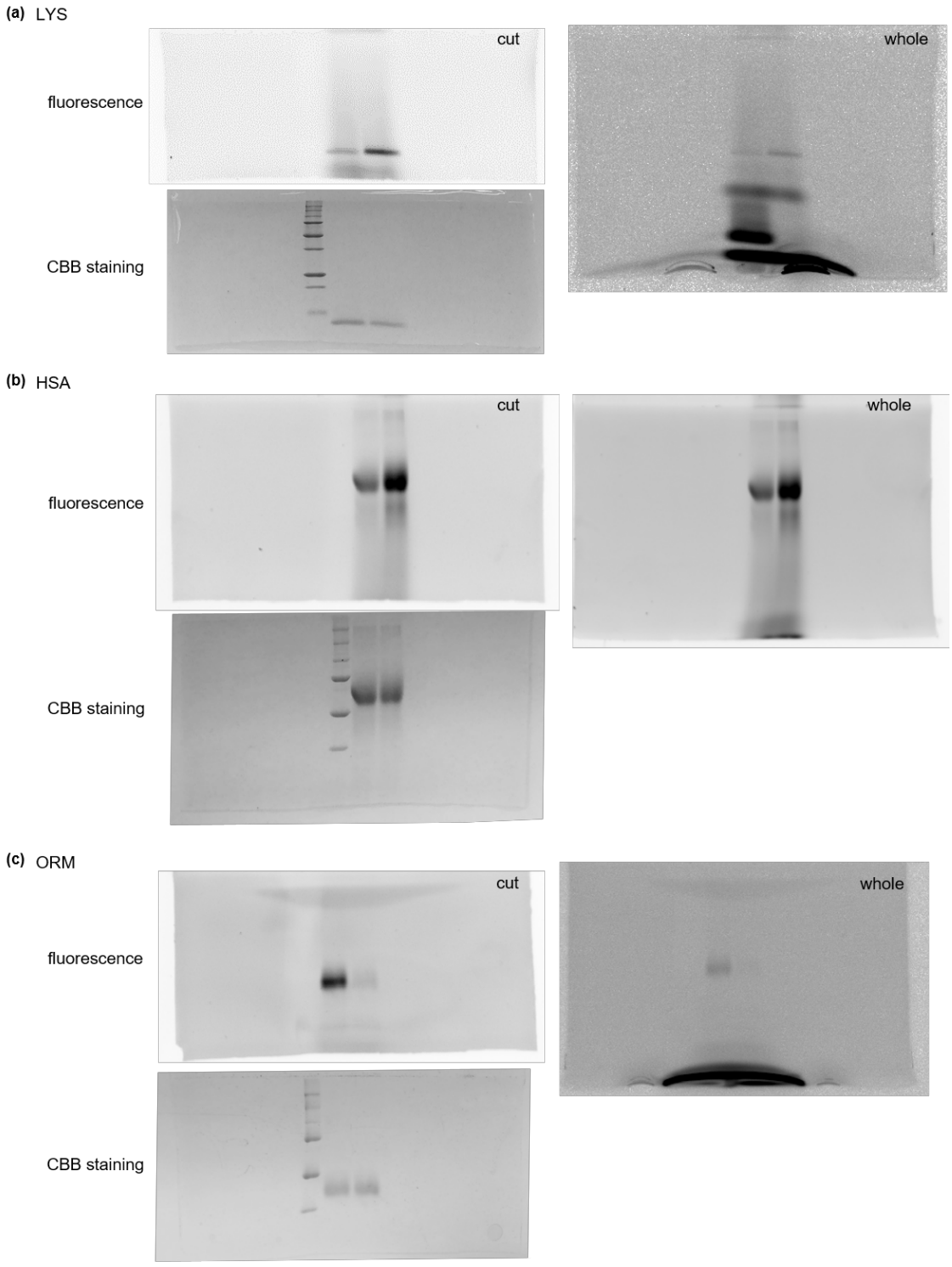

The gel images were used in Fig.3

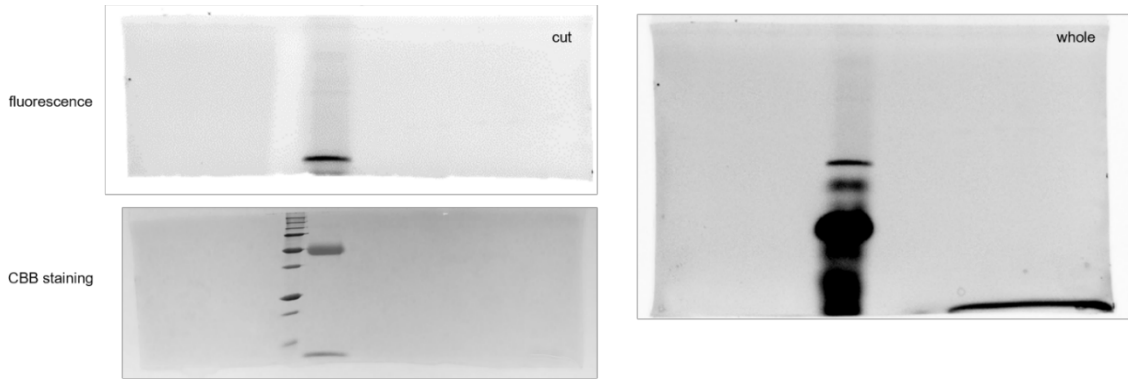

The gel images were used in Fig.4.

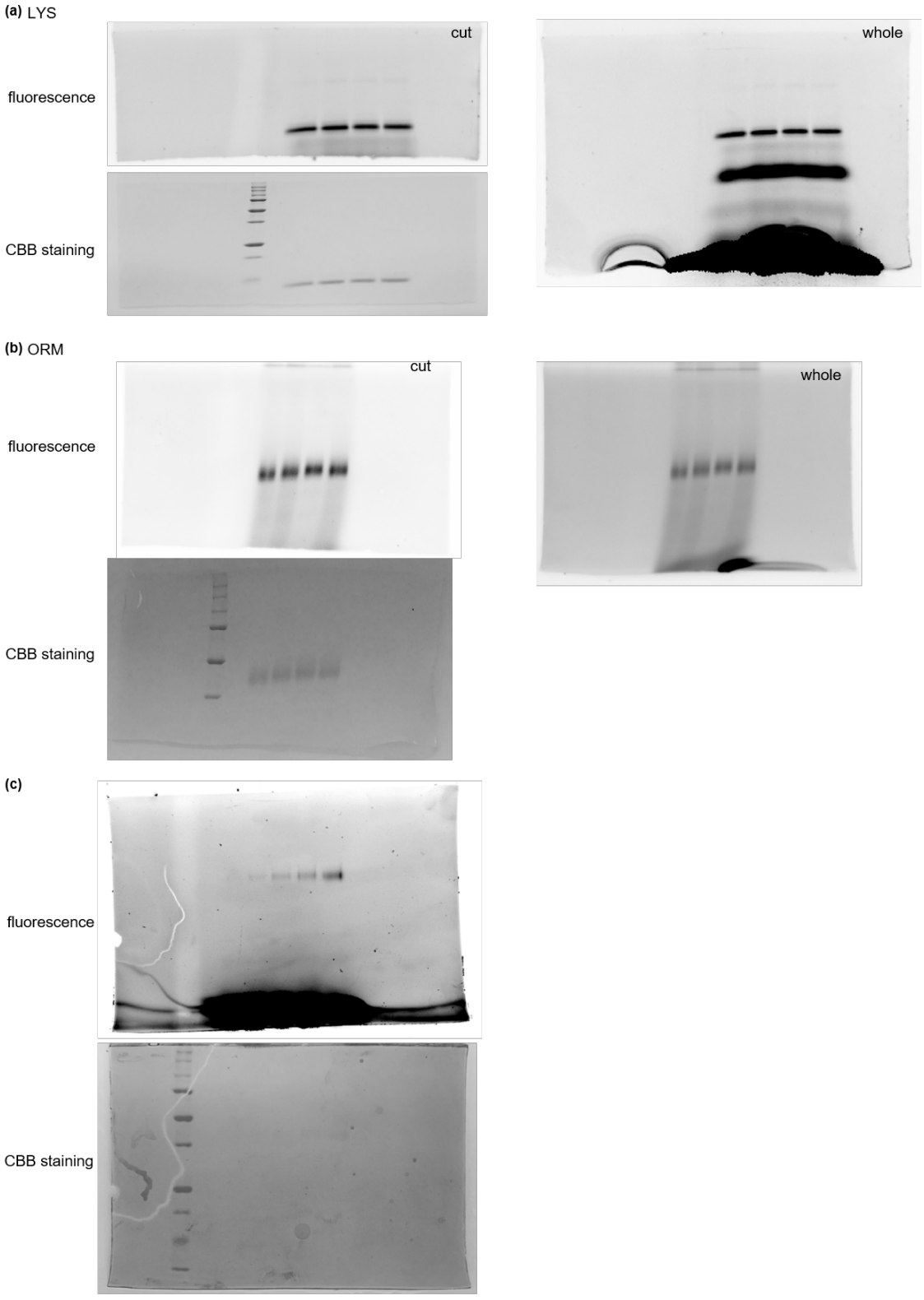

The gel images were used in Fig.S13.